AFML-TR-78-173

LEVEL

IMPACT DAMAGE ON TITANIUM LEADING EDGES FROM SMALL HARD OBJECTS

AD A068458

University of Dayton Research Institute
300 College Park Avenue
Dayton, Ohio 45469
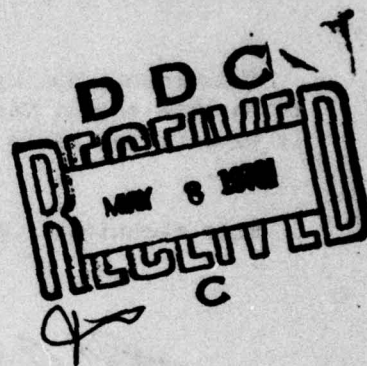
DDC
RECEIVED
MAY 8 1981
C

November 1978

TECHNICAL REPORT AFML-TR-78-173

Interim Report for the period July 1976 to October 1977

AIR FORCE MATERIALS LABORATORY
AIR FORCE WRIGHT AERONAUTICAL LABORATORIES
AIR FORCE SYSTEMS COMMAND
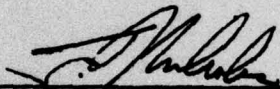WRIGHT-PATTERSON AIR FORCE BASE, OHIO 45433

79 05 07 113

NOTICE

When Government drawings, specifications, or other data are used for any purpose other than in connection with a definitely related Government procurement operation, the United States Government thereby incurs no responsibility nor any obligation whatsoever; and the fact that the government may have formulated, furnished, or in any way supplied the said drawings, specifications, or other data, is not to be regarded by implication or otherwise as in any manner licensing the holder or any other person or corporation, or conveying any rights or permission to manufacture, use, or sell any patented invention that may in any way be related thereto.

This report has been reviewed by the Information Office (OI) and is releasable to the National Technical Information Service (NTIS). At NTIS, it will be available to the general public, including foreign nations.

This technical report has been reviewed and is approved for publication.

THEODORE NICHOLAS, AFML/LLN
Project Engineer

FOR THE COMMANDER

WALTER H. REIMANN, Actg. Chief
Metals Behavior Branch
Metals and Ceramics Division
Air Force Materials Laboratory

SECURITY CLASSIFICATION OF THIS PAGE *(When Data Entered)*

REPORT DOCUMENTATION PAGE	READ INSTRUCTIONS BEFORE COMPLETING FORM

1. REPORT NUMBER	2. GOVT ACCESSION NO.	3. RECIPIENT'S CATALOG NUMBER
AFML-TR-78-173		

4. TITLE *(and Subtitle)*	5. TYPE OF REPORT & PERIOD COVERED
IMPACT DAMAGE ON TITANIUM LEADING EDGES FROM SMALL HARD OBJECTS,	Interim Technical Report. July 1976-October 1977.
	6. PERFORMING ORG. REPORT NUMBER
	UDR-TR-78-54

7. AUTHOR(s)	8. CONTRACT OR GRANT NUMBER(s)
T. Nicholas, AFML John Barber, UDRI Robert S. Bertke, UDRI	F33615-76-C-5124

9. PERFORMING ORGANIZATION NAME AND ADDRESS	10. PROGRAM ELEMENT, PROJECT, TASK AREA & WORK UNIT NUMBERS
University of Dayton Research Institute 300 College Park Dayton, Ohio 45469	Prog. Element: 62102F Task: 241803

11. CONTROLLING OFFICE NAME AND ADDRESS	12. REPORT DATE
Air Force Materials Laboratory/LLN Wright-Patterson Air Force Base OH 45433	Nov 78
	13. NUMBER OF PAGES
	73

14. MONITORING AGENCY NAME & ADDRESS*(if different from Controlling Office)*	15. SECURITY CLASS. *(of this report)*
81 p.	UNCLASSIFIED
	15a. DECLASSIFICATION/DOWNGRADING SCHEDULE

16. DISTRIBUTION STATEMENT *(of this Report)*

17. DISTRIBUTION STATEMENT *(of the abstract entered in Block 20, if different from Report)*

18. SUPPLEMENTARY NOTES

19. KEY WORDS *(Continue on reverse side if necessary and identify by block number)*

Titanium, Foreign Object Damage, Leading Edge Impact Damage, Fatigue Tests

20. ABSTRACT *(Continue on reverse side if necessary and identify by block number)*

Impact damage on titanium leading edge configurations was studied by performing a series of hard particle impact tests and characterizing the damage. Fatigue tests were used to assess the damage and to investigate the applicability of the concept of an equivalent elastic stress concentration factor to characterize severity of damage. Notch fatigue specimens were also fatigue tested in tension to provide baseline data for the titanium material. The data demonstrated reasonable reproducibility and showed that the

DD FORM 1473 EDITION OF 1 NOV 65 IS OBSOLETE

SECURITY CLASSIFICATION OF THIS PAGE *(When Data Entered)*

105 400

20. ABSTRACT (cont'd)

extent of a particular type of damage could be categorized in terms of an equivalent elastic stress concentration factor. The fatigue test results also showed that the damage sustained from very small particles, which completely perforated the leading edge and removed material was essentially the same in terms of fatigue strength as a machined notch of the same geometry.

The concept of geometric scaling was investigated by performing a series of impact tests using different leading edge thicknesses and projectile sizes. Observation of the type of damage, and plots of critical velocity versus particle size (in relation to leading edge thickness) appeared to validate the scaling concepts.

FOREWORD

ACCESSION for
NTIS   White Section
DDC   Buff Section
UNANNOUNCED
JUSTIFICATION

BY
DISTRIBUTION/AVAILABILITY CODES
Dist.   SPECIAL

A

79 05 07 113

TABLE OF CONTENTS

LIST OF ILLUSTRATIONS

SECTION I
INTRODUCTION

Fan and compressor blades in jet engines are subjected to damage from foreign objects ingested with the air into the engine. The blades are exposed to potential impacts from a variety of objects ranging from large birds to small particles of sand. The engine speed, blade material, blade geometry, point of impact, and type and size of impacted object all play important roles in determining what type, if any, and the severity of damage which might occur. In addition, damage may be immediate causing instantaneous fracture or failure, or may be of the type that could lead to eventual failure through fatigue crack initiation or growth to a catastrophic size. Because of the large number of parameters involved and the near impossibility of determining the cause or source of service induced damage, it is not surprising to find little, if any, information of a quantitative nature on impact induced damage in fan or compressor blades, especially from small hard particles.

Compressor blades can be especially susceptible to damage from ingested small hard particles such as sand or stones because of the large quantity of such particles in the environment and the thin leading edges of these blades. Leading edge thicknesses of 0.010" (0.25 mm) or less are common in the compressor stages of todays high performance engines. Titanium alloys such as Ti 6Al-4V(6-4) or Ti 8Al-1 Mo-1V (8-1-1) are commonly used in such applications. In-service inspections of such blades occasionally reveal damage in the form of small nicks, dents, or bulges, which can lead to complete blade failure due to the propagation of fatigue cracks from the damaged area. Visual inspection of blades nicked or damaged along the leading edge does not permit accurate determination

1

of the size and type of object that might have caused the damage. Conversely, the designer wanting to know what type of damage might be sustained from a given object such as a specific size sand particle would have no source of such information. Even the empirical testing of a blade is difficult because the capability to hit a blade with a small sand particle at velocities which occur in a rotating stage of a jet engine cannot be considered state-of-the-art.

Because of the lack of information on small hard particle impact damage in blades, and because of some unanswered questions involving damage sustained in engine tests, a program was undertaken to evaluate the damage produced by such particles impacting on typical leading edge configurations. As a prerequisite for this study, experimental capability had to be developed and demonstrated to perform the required tests. This report presents the results of a study on small hard particle impact damage in 8-1-1 Ti leading edge configurations. Numerous parameters were investigated in this program. The work, in no way complete, serves as guidance for future work in this area and provides a basis for a rational approach to the study of this type of foreign object damage.

2

SECTION II
EXPERIMENTAL PROGRAM

The experimental program was broken up into a number of phases, each of which is described in detail in a subsequent section. The scope of the program involved performing impact tests on typical leading edge configurations using small hard particles in the size range 0.020" to 0.065" (0.51 to 1.65 mm) diameter at velocities ranging from 400 to 1600 ft/s (120 to 490 m/s) which covers typical operating conditions of a number of engine compressor stages. The impact velocity is obtained from the vector sum of the rotational speed of the engine and the forward velocity of the aircraft, assuming the impacted projectile to be essentially at rest. The angle of impact is obtained in a similar manner using vectors and taking into account the pitch of the blade. For all of the tests performed here, an impact angle of 30° with the plane of the blade was used arbitrarily. In an actual engine, this angle could vary from nearly 0° or a head-on impact to over 40°. The material chosen for this study was again arbitrary, 8-1-1 Ti sheet in .063" (1.6 mm) thickness being selected on the basis of availability more than anything else. No attempt was made to simulate any particular blade or material microstructure.

The first two phases of the program were run concurrently. The first phase, described in Section III, involved characterizing the baseline titanium material in terms of notch fatigue strength. The second phase, described in Section IV, involved developing an experimental technique to impact leading edge specimens under specified conditions, designing of the specimen and fixtures, and performing several impact tests to evaluate damage. Parameters such as projectile type, size, velocity, impact angle, and temperature were all looked at briefly to try to scope the extent of the induced damage and

3

the significance of the various parameters. The next series
of tests involved choosing several impact conditions, impacting
a batch of specimens under each condition, and then fatigue
testing each batch for comparison with the baseline notch
fatigue data for the test material. These tests are described
in Section V. Following this, the effect of particle material
and shape and impact velocity was investigated in a matrix of
impact experiments. These tests are described in Section VI.
Included here also was a series of tests involving impacting
single particles of debris from a wind tunnel for comparison
with damage induced by known particles. Finally, Section VII
describes a matrix of test shots in which the concept of geo-
metric scaling was investigated. Here, leading edge thicknesses
up to .030" (.76 mm) and projectiles up to .250" (6.35 mm)
diameter were used.

In all impact experiments, the damage was measured, des-
cribed, and photographed. The tables of test conditions and
photographs of damage are presented in the Appendix.

4

SECTION III
MATERIAL CHARACTERIZATION

Ti 8Al-1 Mo-1V (8-1-1) was selected arbitrarily as the baseline material for all tests in this program. A single sheet, .063" (1.6 mm) thick, was used for all specimens to assure uniformity in material properties from test to test. All specimens were cut in the same direction in the sheet to avoid any preferred orientation effects in the sheet. This particular titanium was chosen as being representative (in terms of modulus, density, and strength characteristics) of alloys commonly found in compressor blades in jet engines but was not meant to represent any particular blade in any specific engine; it was simply chosen as a model material to work with.

Notch fatigue specimens were machined from 6" x 1-1/2" (152 x 38 mm) blanks cut from the titanium sheet to the dimensions shown in Figure 1. Six specimens of each type were machined, having elastic stress concentration factors of 1.45, 2.20, and 3.72. The specimens were then fatigue tested in tension in a 5 ton (44.5 KN) Shenck Resonant Fatigue Testing Machine using a ratio of minimum load to maximum load (R ratio) of 0.1. The cyclic frequency of the Shenck machine is approximately 33 Hz. The number of cycles to failure (complete separation) was recorded for each specimen. No attempt was made to correct for the number of cycles necessary to propagate from the first observable crack to failure; in all cases this was small compared to the total cycles. The data for the three groups of specimens are plotted as N_f (number of cycles to failure) versus maximum net section stress in Figure 2. A straight line was drawn for each group of data and was used, subsequently, as the baseline representation of the notch fatigue strength of the test material.
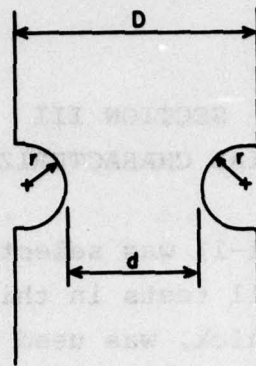
Type	D(mm)	d(mm)	r (mm)	K_T
I	36.4	29.7	12.7	1.45
II	36.4	29.7	3.2	2.20
III	36.4	29.7	0.8	3.72

Figure 1. Geometry of notch fatigue specimens.
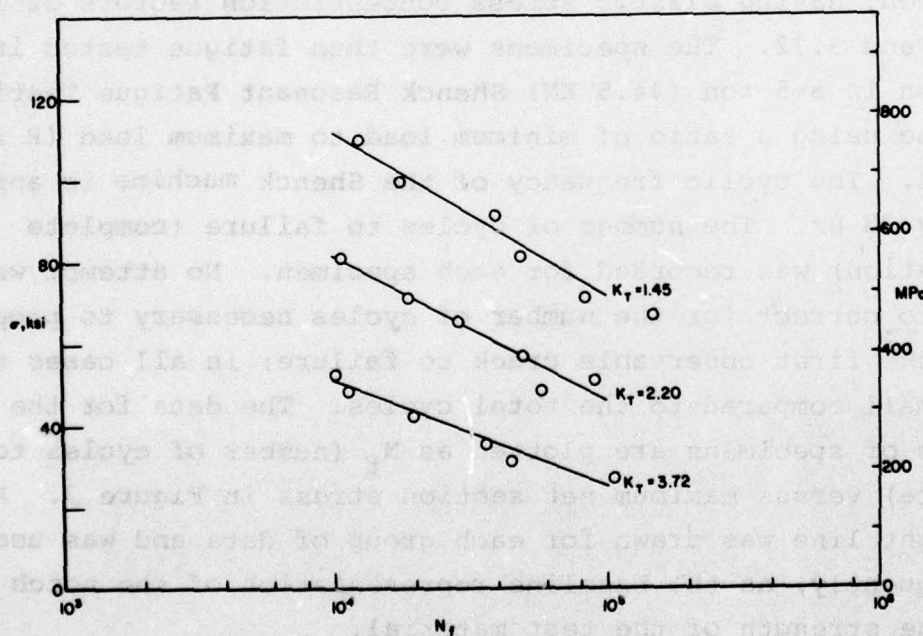
**Figure 2. Baseline notch fatigue data for Ti 8-1-1 sheet
(1/16" thick).**

To further characterize the baseline material, three single notch crack growth specimens were fabricated to nominal dimensions of 2-1/4" x 9" (57 x 228 mm) and tested in an MTS servo hydraulic test machine at a frequency of 20 Hz, again using an R ratio of 0.1. The raw data of crack length, load, and number of cycles were reduced to values of $\Delta a/\Delta N$ and stress intensity factor, K, and plotted as da/dN versus K_{max} in Figure 3.
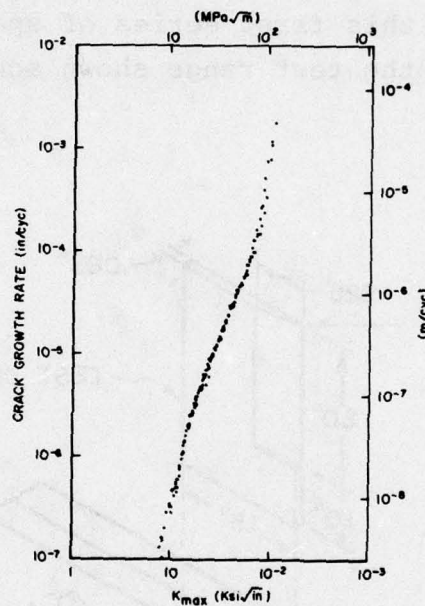
Figure 3. Crack growth rate in 1/16" Ti 8-1-1 sheet using single edge notch specimen.

SECTION IV
IMPACT TEST SET-UP AND EXPERIMENTAL RESULTS

Test specimens having leading edge thicknesses of approxi-
mately .010" (.25 mm) and a nominal 5° taper angle were machined
from the titanium sheet and mounted as shown in Figure 4. The
thickness of the leading edge was held between .008" (.20 mm)
and .010" (.25 mm) for this first series of specimens. The
fixture was mounted in the test range shown schematically in
Figure 5.
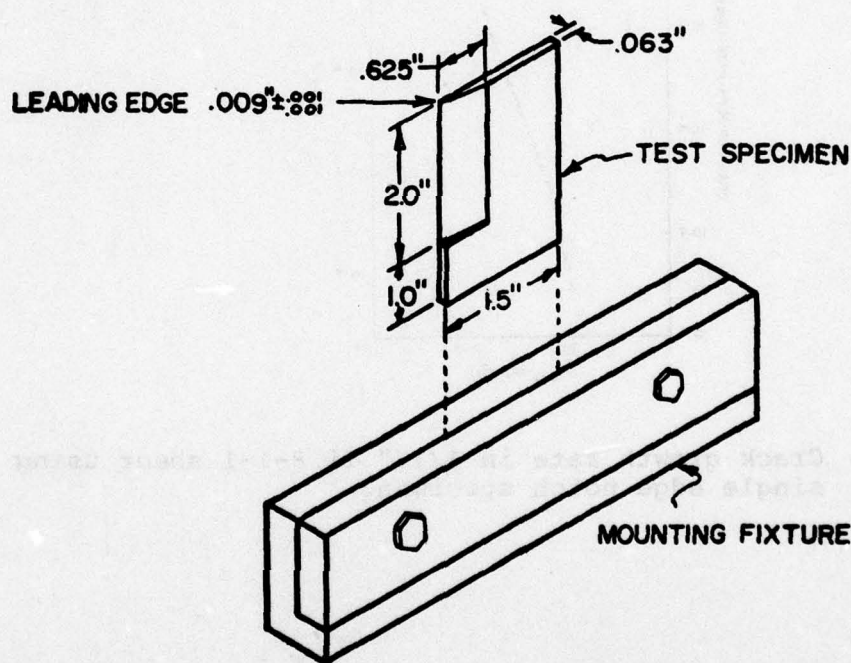
Figure 4. Tapered-edge test specimen and mounting fixture.

The range set-up consists of a launch tube, velocity
measuring system, and a target tank with a mounting fixture. The
launch tube has a smooth bore of 0.305" (7.75 mm) and a length
of 3'(1 m). The projectile particles to be fired were positioned

8
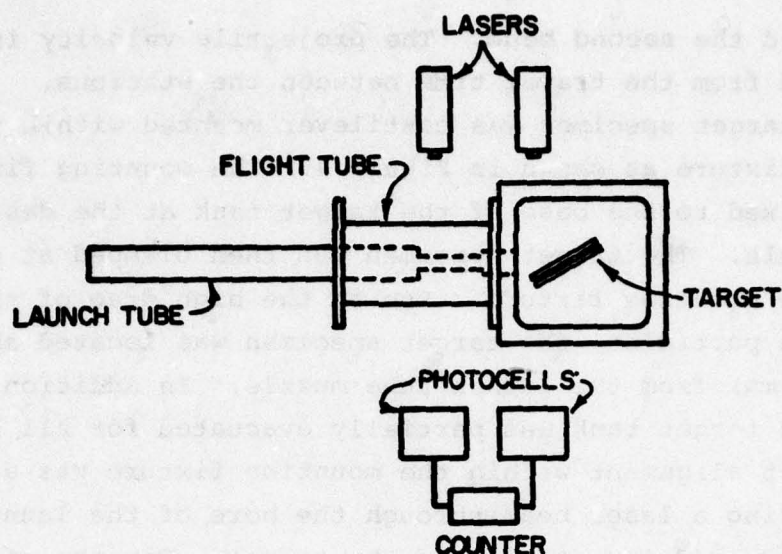
Figure 5. Schematic of range set-up.

into a recessed pocket of a lexan sabot to provide protection
and support for the particles during launch. The particles were
held within the pocket by an oil film during the launch. The
projectile particles/sabot package was launched down the tube
by utilizing either compressed gas or powder gas depending on
the desired impact velocity. Compressed gas was used for
impact velocities up to 1000 ft/s (305 m/s). Above 1000 ft/s
(305 m/s) a powder gun was used. A sabot stopper device was
located at the muzzle of the launch tube. The purpose of this
device was to slow down and eventually stop the sabot, per-
mitting the particles to separate from the sabot and continue
on a trajectory towards the target specimen.

The projectile velocity was measured by utilizing a pair
of HeNe laser/photomultiplier stations spaced a known distance
apart. Each laser beam intersects the projectile particles
trajectory normal to the trajectory and illuminates one of the
photomultiplier stations. When the projectile/sabot package
interrupts the first beam (first station had laser beam pro-
jecting through slots at muzzle of launch tube), the first
photomultiplier station generates a voltage pulse to start a
counter-timer. The counter-timer is stopped when the particles

9

interrupted the second beam. The projectile velocity is then
calculated from the travel time between the stations.

The target specimen was cantilever mounted within the
mounting fixture as shown in Figure 4. The mounting fixture was
rigidly fixed to the base of the target tank at the desired
impact angle. The target specimen was then clamped at one end
within the mounting fixture. Due to the high drag of the small
projectile particles, the target specimen was located about
4.0" (102 mm) from the launch tube muzzle. In addition, the air
within the target tank was partially evacuated for all impacts.

Target alignment within the mounting fixture was achieved
by projecting a laser beam through the bore of the launch tube
onto the desired impact site of the target. For the case of
edge impacts, the target was positioned such that the laser
beam was split by the target edge at the desired impact site.

After a preliminary series of tests to establish the
necessary gas pressure or powder charge to achieve a given
velocity, a series of leading edge impacts were conducted using
either glass beads or silica sand particles as the projectiles.
The impact velocities of the tests were either 1000 or 1500 ft/s
(305 or 458 m/s). Thirty-four of the tests were conducted at
angles of incidence of 30°, ten tests at 10° impact angles, and
the remaining four tests at 30° impact angles with the test
specimens at 250°F temperature, to investigate the effect of a
slightly elevated temperature on the damage. The data from the
preliminary set-up tests (#8299-8308) and the first series out-
lined above (#8309-8356) are summarized in Table 1. This
table, and subsequent ones, provides the shot number, test
specimen material and type, thickness at impact site (leading
edge thickness), support method (cantilever in all these tests),
projectile type, size, and velocity, type of impact including
impact angle, location of impact and temperature if other than
room temperature, and finally a visual description of the damage
generated on the test specimen under "remarks".

This first series of tests involved multiple impacts on the
target since several particles were placed in the sabot for each

10

shot. At the beginning of the test program, it was not known how accurately the small particles could be launched or how far off trajectory they would spread, hence a shotgun approach was used to increase the probability of hitting the leading edge.

Several things were observed from the results of this series of tests. First, observations of the post-test tapered-edge specimens indicated that silica sand impacts caused more severe damage than glass beads, probably due to their generally irregular shape. Second, impacts by glass beads less than 0.020" (0.51 mm) produced very little damage on the specimen surface. These very small particle impacts generated a peened or pitted surface on the tapered edge of the specimen without material loss. At higher velocities (1500 ft/s (458 m/s) a very small amount of plastic deformation could be observed. It was concluded that impacts of particles under 0.020" (0.51 mm) size does not appear to be a threat to blades of titanium in the velocity range up to 1500 ft/s (458 m/s).

Two other facts were evident from this first series of tests upon observation of the impacted specimens. There appeared to be no observable difference in the induced damage under the conditions noted when (a) the impact angle was changed from 30° to 10° and, (b) the temperature was raised from room temperature (70°F) to 250°F.

Other observations were, as one would expect, that the amount of damage or the size of the area of plastic deformation increases with increasing velocity and with increasing particle size. It should be noted here that the particle size varied from 0.005 to 0.063" (0.13 to 1.6 mm) diameter and the velocity from approximately 1000 to 1600 ft/s (300 to 490 m/s). Also, it was noted that the impacts from silica sand appeared to cause a greater amount of plastic deformation than similar impacts with glass beads.

Material removal from the edge of the specimens was predominant for both glass and silica sand impacts for particle sizes above 0.020" (0.51 mm) diameter. Photographs of typical damage showing material removed are shown in Figures 6 through 12.

11
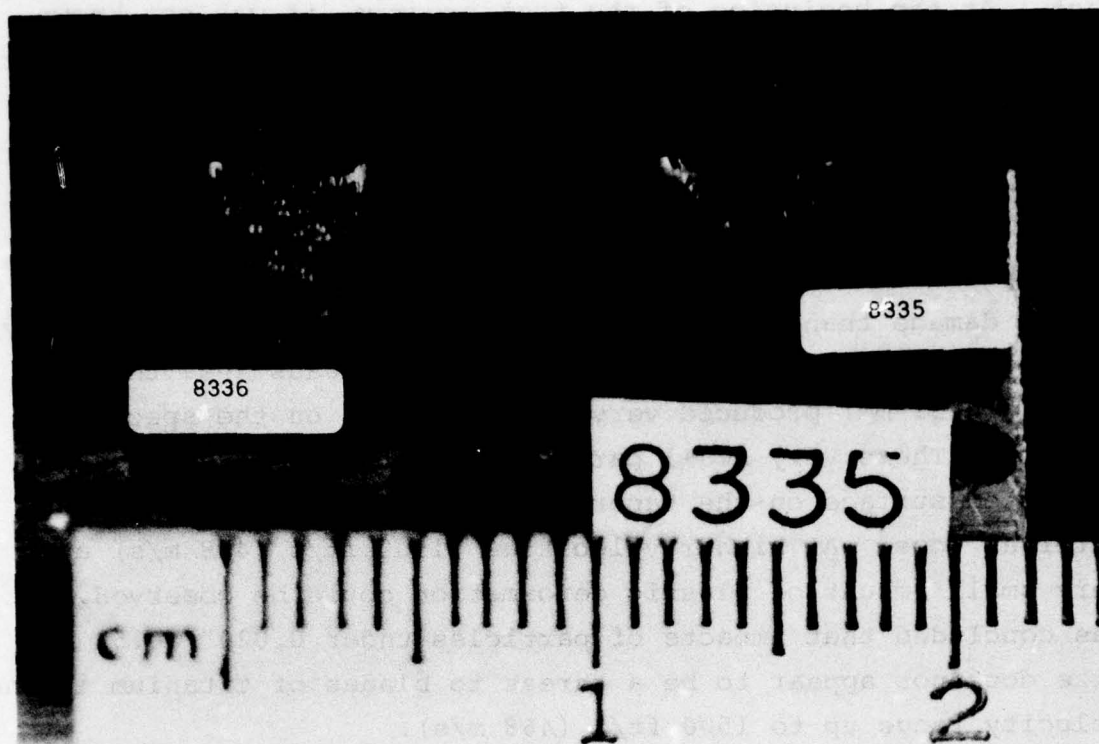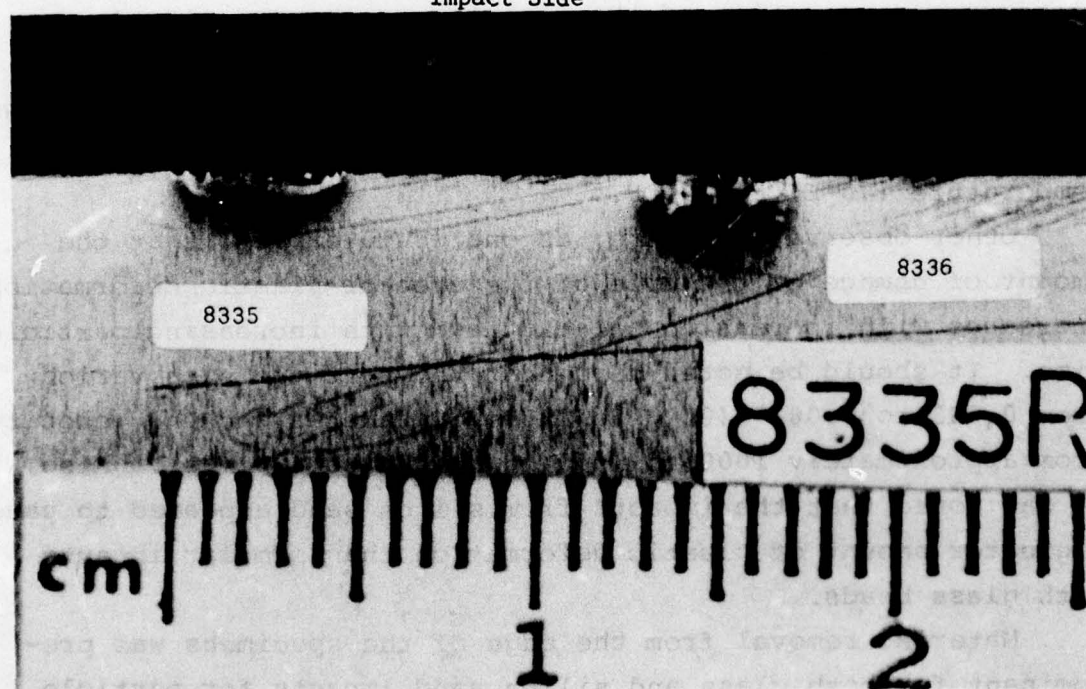
Impact Side

Exit Side

Figure 6.   Photographs of damage due to glass bead impacts at 30° (Shots 8335 and 8336).

12
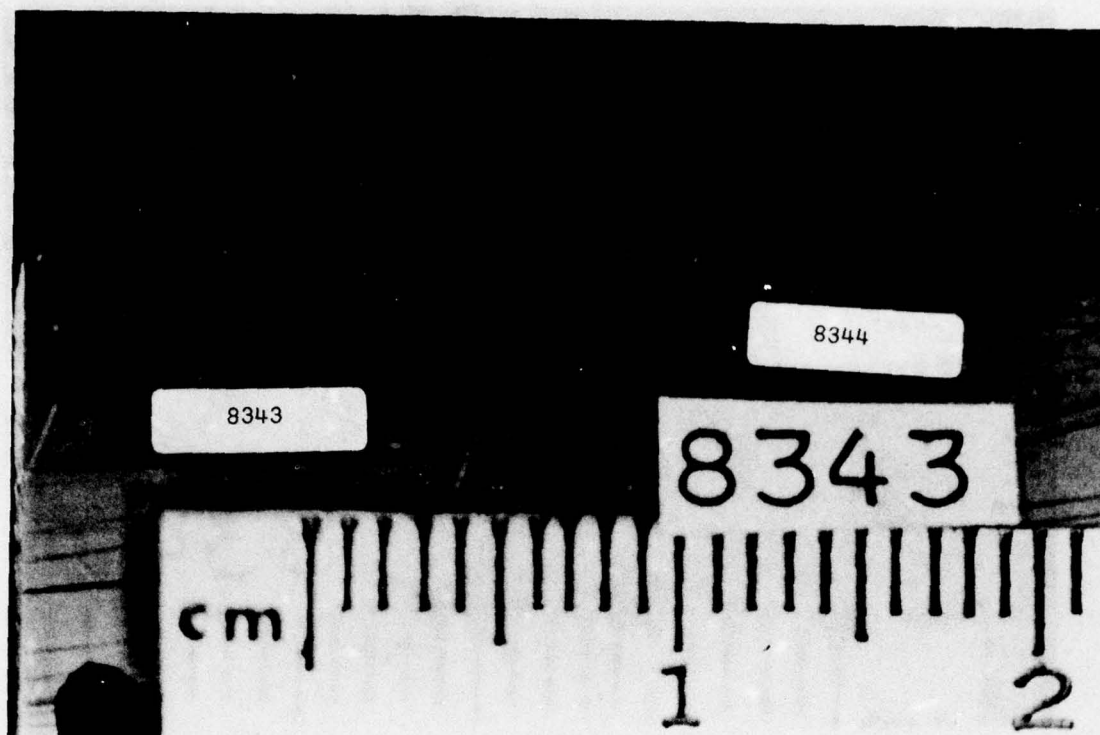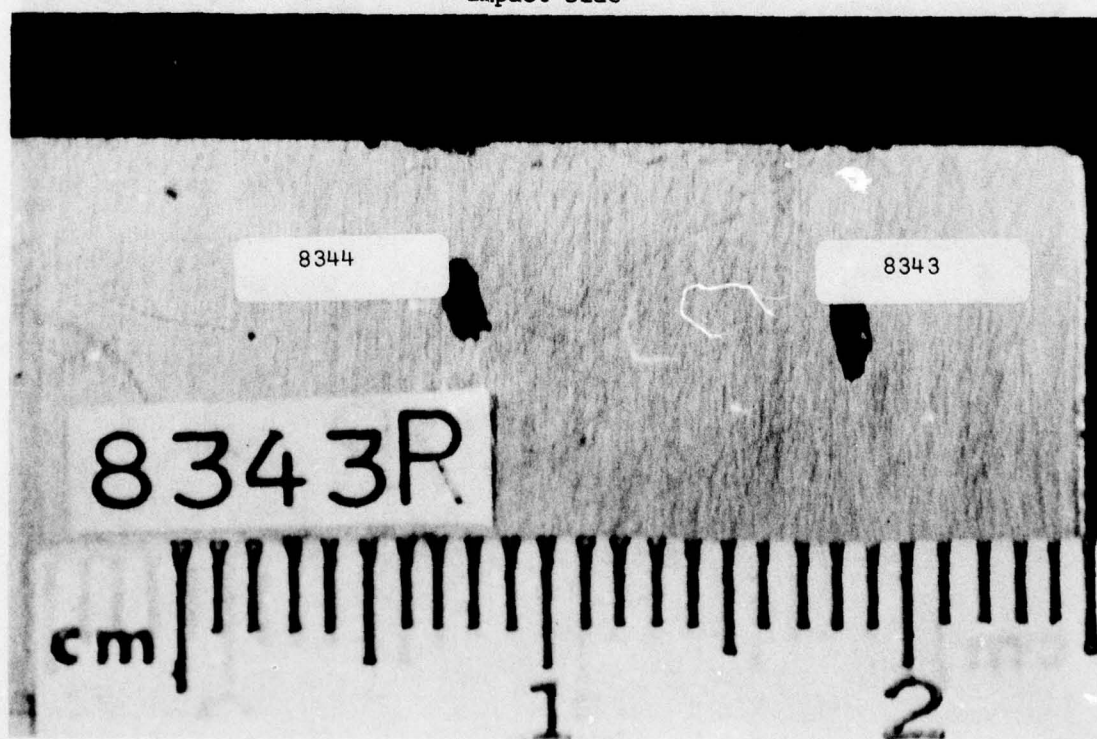
Impact Side

Exit Side

Figure 7. Photographs of damage due to glass bead impacts at 10° (Shots 8343 and 8344).
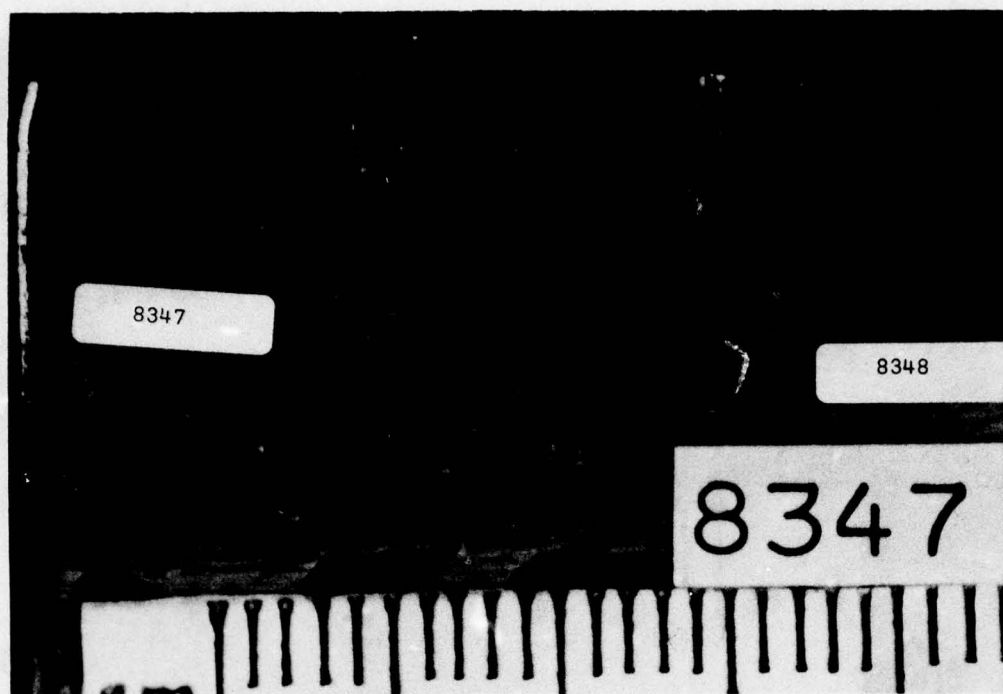
Impact Side
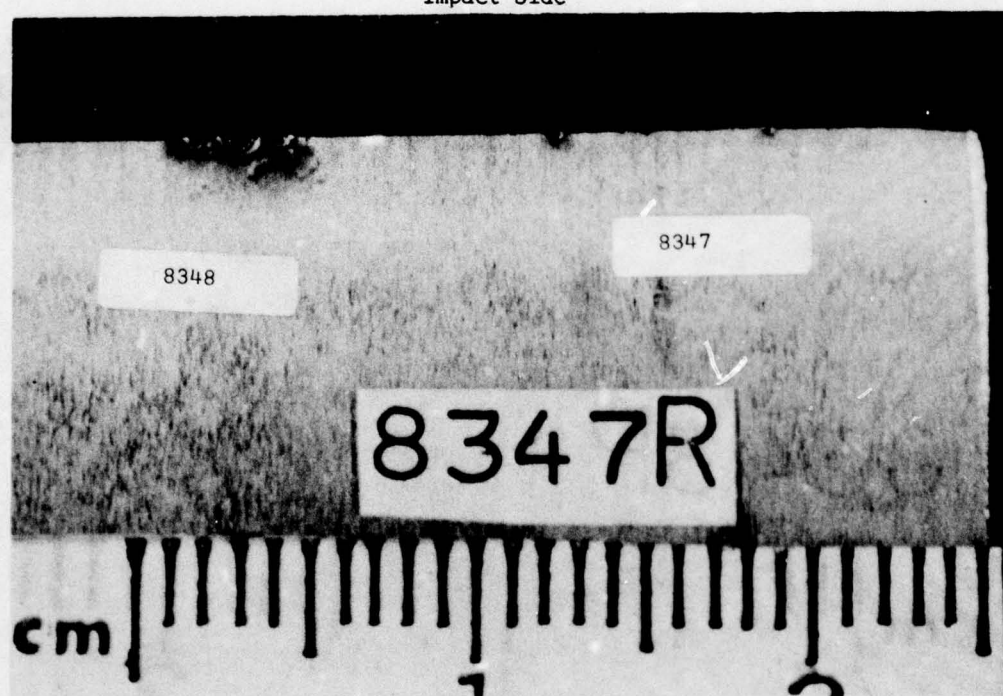
Exit Side

Figure 8. Photographs of damage due to glass bead impacts at
30° and 250°F (Shots 8347 and 8348).
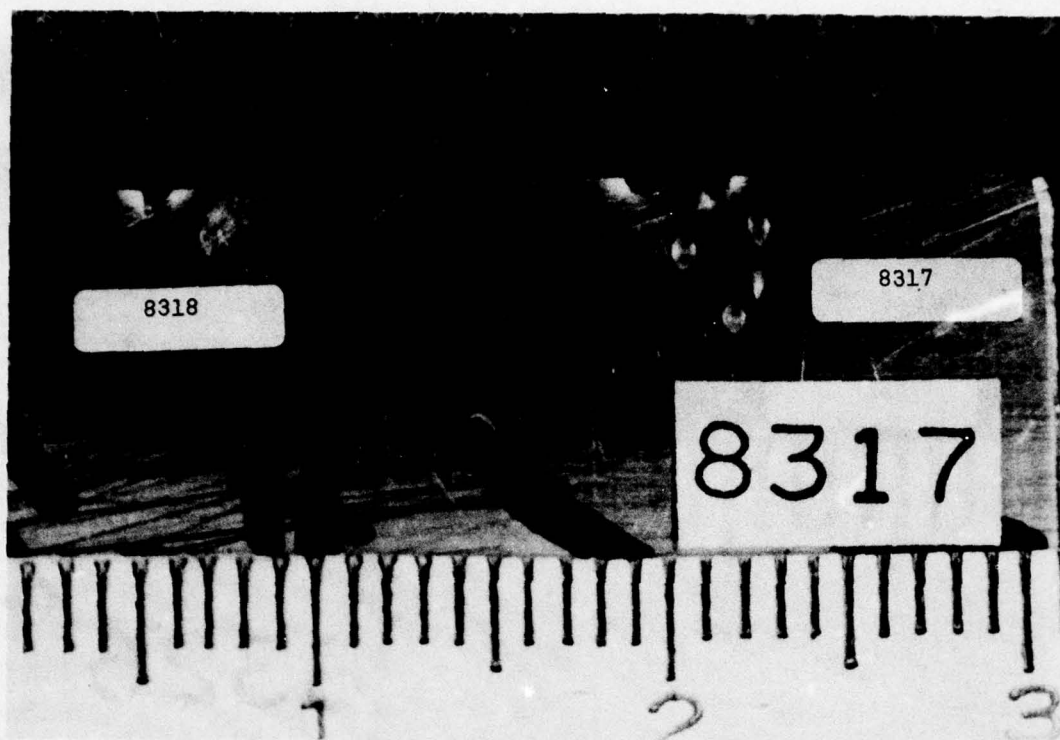
Impact Side
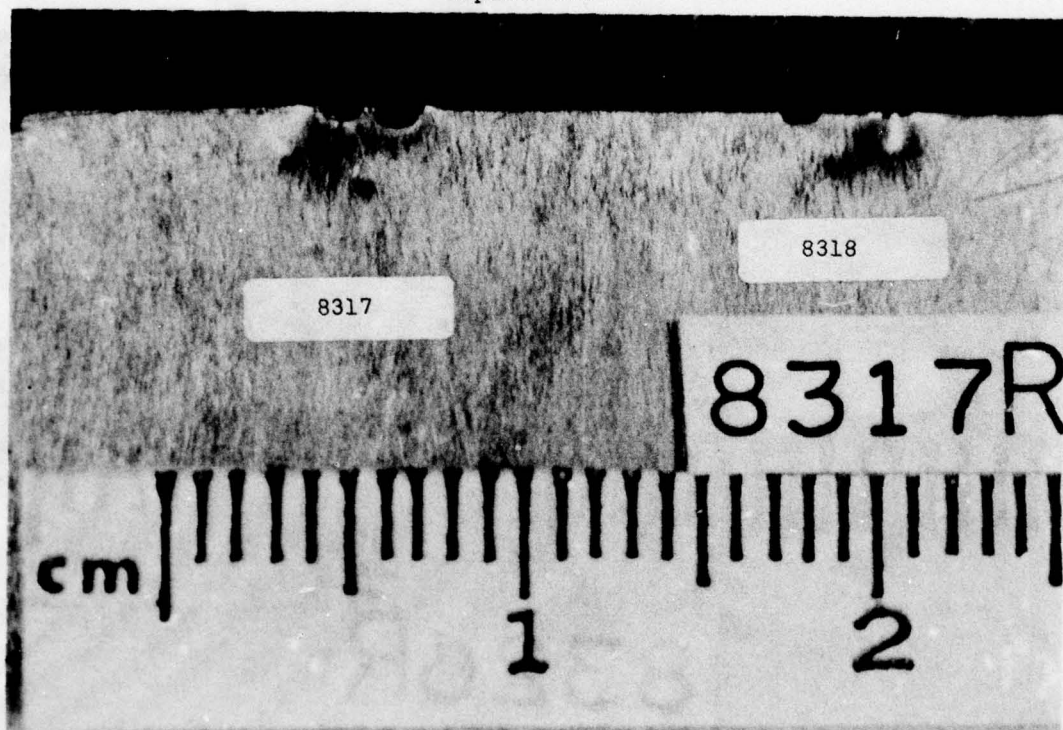
Exit Side

Figure 9. Photographs of damage due to Pyrex bead impacts at
30° (Shots 8317 and 8318).

15
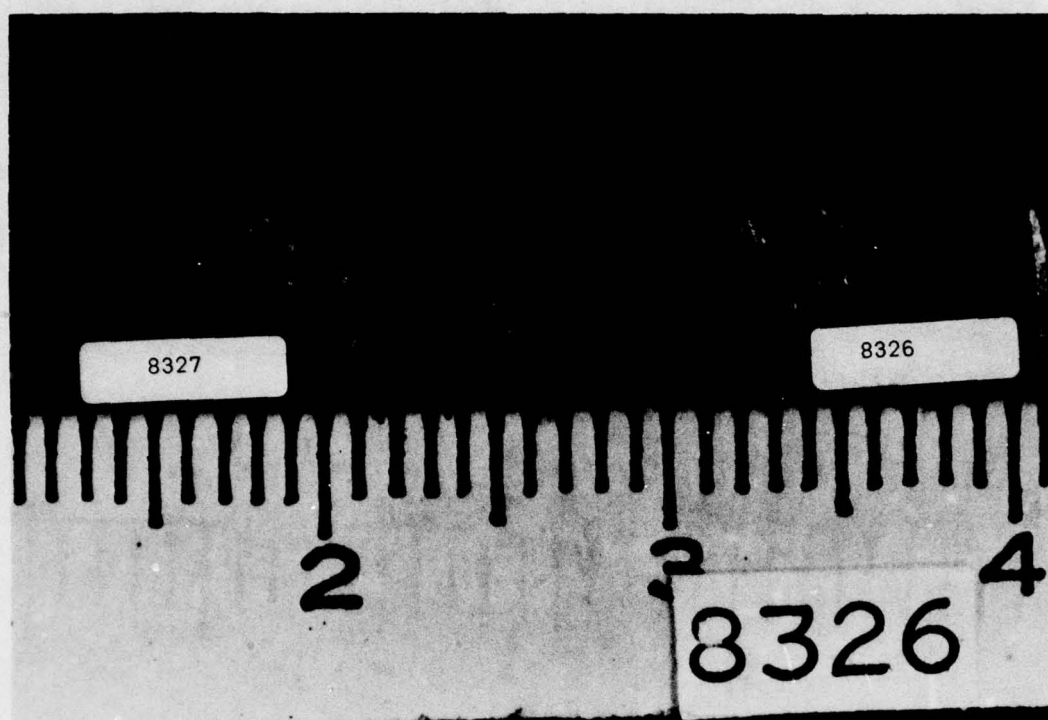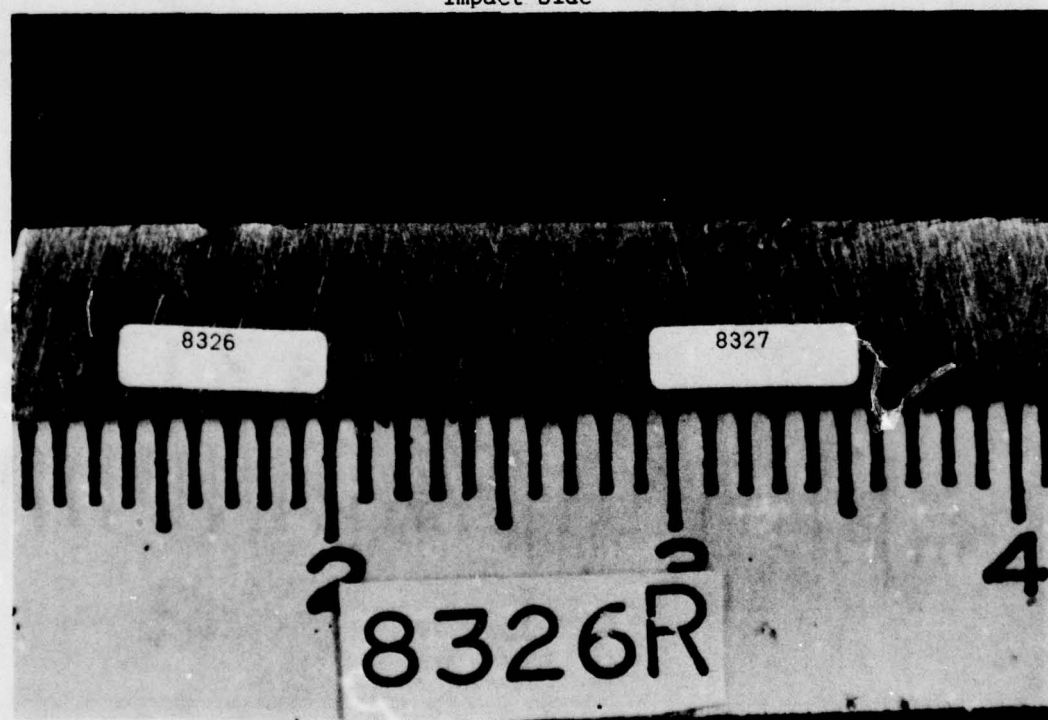
Impact Side

Exit Side

Figure 10. Photographs of damage due to silica sand impacts
at 30° (Shots 8326 and 8327).

16

8322
Impact Side

8322R
Exit Side
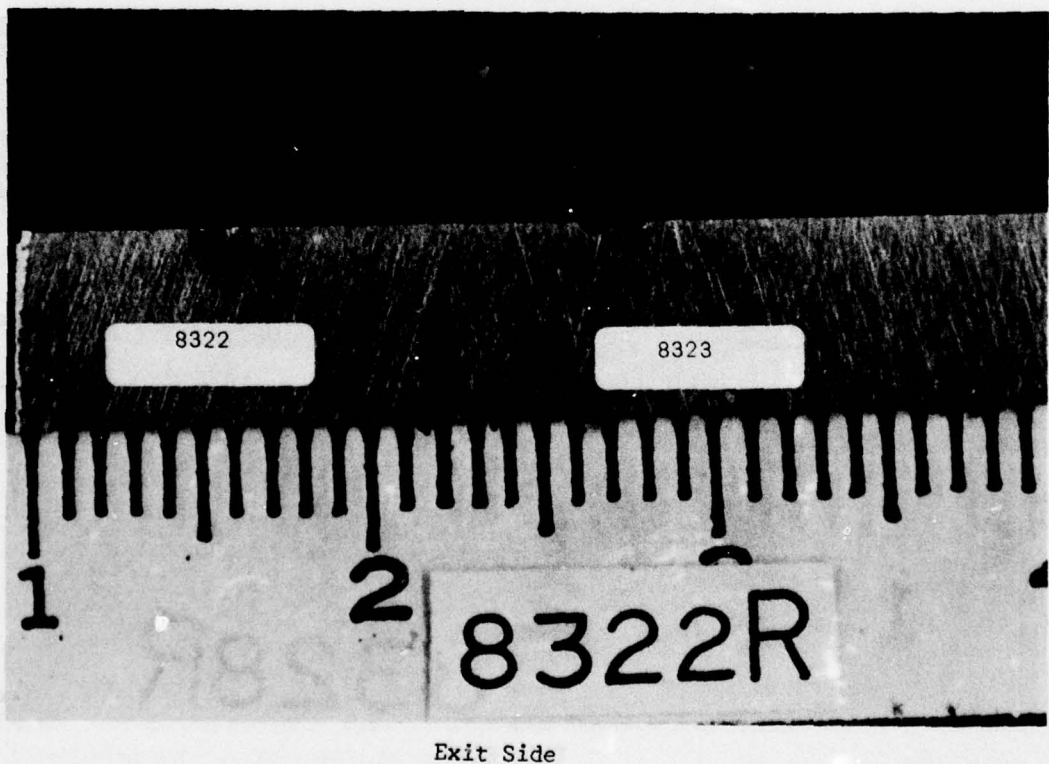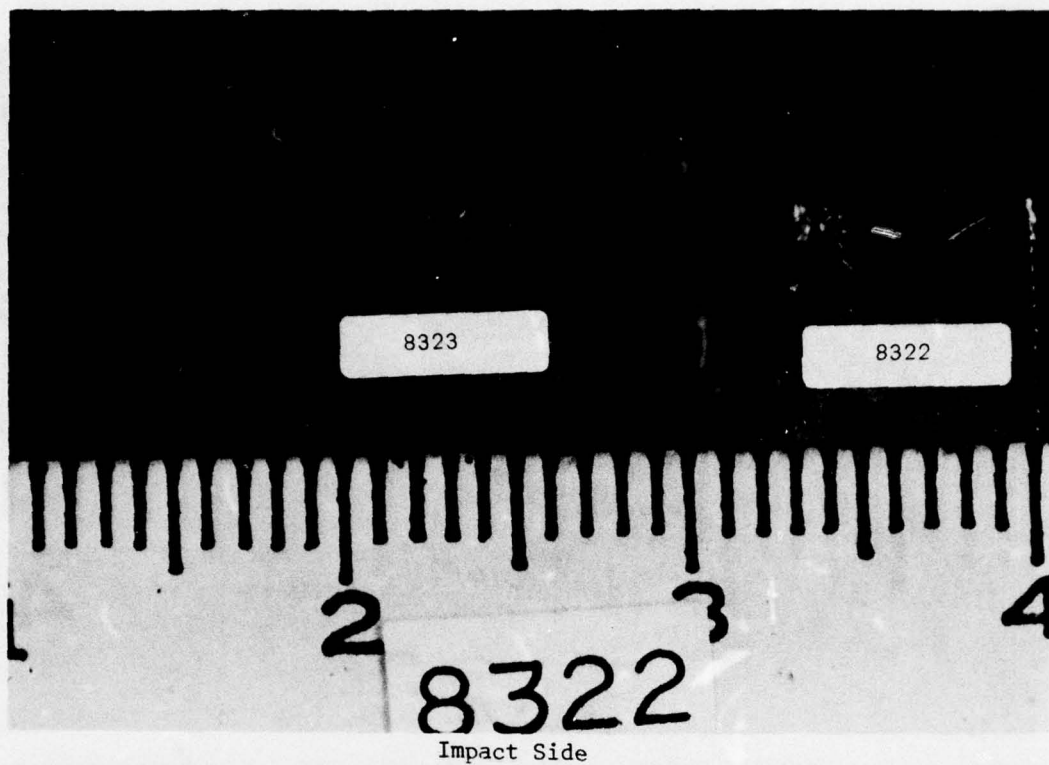
Figure 11. Photographs of damage to silica sand impacts at 30° (Shots 8322 and 8323).

Impact Side

Exit Side
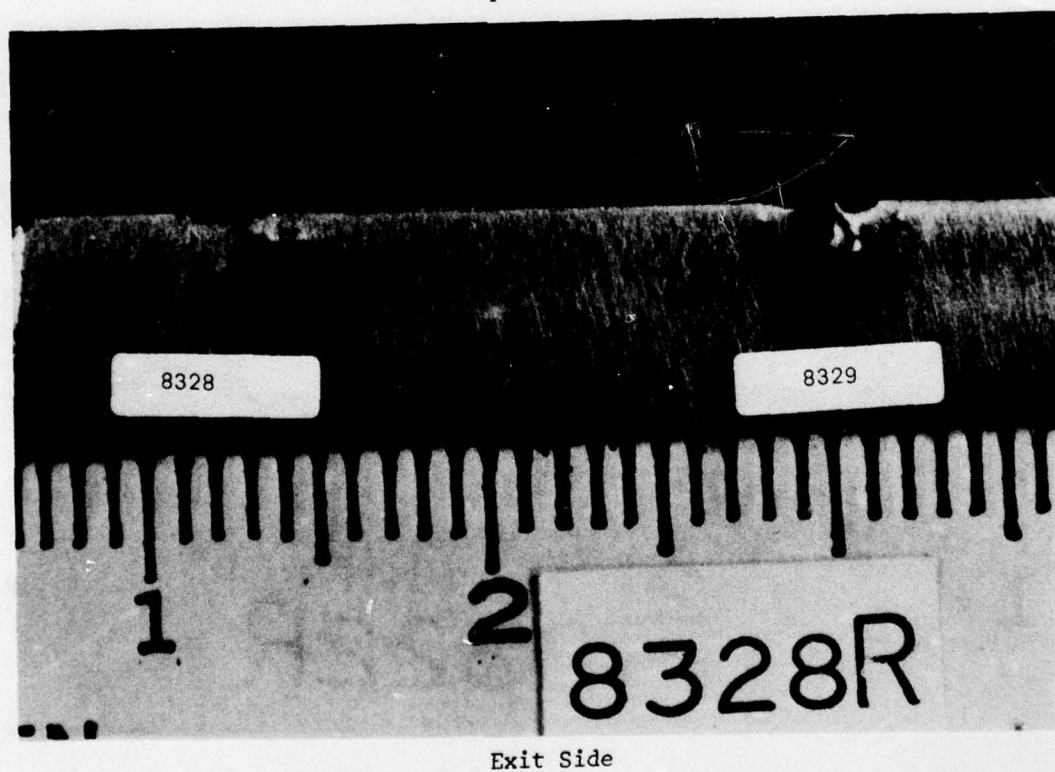
Figure 12. Photographs of damage due to silica sand impacts at 30° (Shots 8328 and 8329).

18

Note that the shape of the holes or material removed approximates the diameter or portion of particle impacting the edge of the test specimens. For instance, if the trajectory of a particle was such that only a small portion of the particle impacted the specimen edge, only a small amount of material was removed and the shape of the hole was similar to the impacting portion of the particle. If a particle had a trajectory such that half of the particle impacted the specimen edge, the resulting perforation was semicircular in shape.

From the results of this phase of testing, it was determined that damage to 0.010" (0.25 mm) leading edge titanium blades could result from sand particles in the size range from 0.020" (0.51 mm) diameter and larger at velocities typical of those encountered by compressor blades in jet engines. It was also determined that typical damage could be inflicted upon thin leading edge specimens by small particles launched in a laboratory experimental set-up.

SECTION V
FATIGUE STRENGTH OF IMPACTED SPECIMENS

Having established a technique for impacting leading edge specimens with small hard particles, it was important to develop some quantitative measure of damage. Measurements of damaged specimens were made to determine the depth and width of the resulting dent, crater, or perforation and also the extent of the significance of the damage with respect to blade function. The concept decided upon was to describe the damage in terms of an equivalent stress concentration factor and/or an equivalent crack length. From this the residual fatigue and tensile strength of the specimen (or blade) could be determined. To investigate the concept of an equivalent stress concentration factor, a series of fatigue tests was conducted using groups of specimens impacted under identical conditions. To further control the damage, each specimen was impacted with a single particle.

Impacts were conducted with three different size particles at approximately the same velocity and at a higher velocity for the intermediate size particle. All the particles were spheres of glass or Pyrex. Because of the launch technique used and the characteristics of powder guns, the velocity of each shot could not be accurately reproduced. The actual velocities and test conditions are presented in Table 2. The nominal particle sizes and velocities were 0.062" at 1600 ft/s (1.6 mm, 490 m/s), at 1100 ft/s (1.6 mm, 340 m/s), 0.125" at 800 ft/s (3.2 mm, 240 m/s), and 0.030" at 1000 ft/s (0.8 mm, 300 m/s).

Leading edge specimens were made from 6" long by 1-1/2" wide (152 x 38 mm) blanks cut from a titanium sheet. A leading edge with a taper of 4 degrees was ground onto the center 1" (25 mm) portion of the specimen over half the width. Each specimen was impacted by a single particle launched with a lexan sabot. For

the very small particles, a small depression was made at the bottom of the sabot and the particle was placed in it and held in place with a small drop of light oil. The center of the specimen leading edge was aligned with the centerline of the launch tube for each shot. For the very small particles, however, it was not always possible to impact the center of the leading edge because of slight unpredictable drift in the trajectory. In these cases, one or more shots were used to achieve a series of similar leading edge impacts. A minimum of six specimens were impacted under nominally identical conditions for each of the four combinations of particle size and velocity.

Each group of specimens with assumed identical damage was fatigue tested in a Schenck resonant tensile fatigue machine using an R ratio of 0.1. The load levels were chosen to produce failure in the range from 10^4 to 10^5 cycles, the same region in which the baseline notch fatigue data were obtained for the titanium material used for all the specimens. For each group of specimens, data were plotted in the form of net section *average stress against number of cycles to failure.* It must be emphasized here that net section stress was used in all the plots. The net cross-section is the product of the 0.063" (1.6 mm) thickness by the 1-1/2" (38 mm) width, less the area removed in tapering the specimen down to the leading edge thickness. No correction was made for the area removed due to the impact. Note also that the cross-section is not uniform along the length of the specimen since the leading edge geometry is machined along only the center 1" (25 mm) of the total 6" (152 mm) length. Stress concentrations of an undetermined magnitude thus occur along the leading edge. An attempt was made to determine the stresses along the leading edge in the fatigue test by attaching strain gages to the specimen at various positions on the cross-section at the mid-length location. However, no consistent readings could be obtained. It was generally observed, however, that the axial stress near the leading edge was somewhat higher than the average stress across the cross-section.

21

The data points for the four impact conditions are presented in Figures 13-16 in the form of plots of average net-section stress, σ, against number of cycles to failure, N_f. For reference purposes only, the three curves corresponding to the baseline notch fatigue data for this titanium for $K_T = 1.45$, 2.20, and 3.72, are superimposed on each of the plots. This simplifies comparison of one set of data with another. Note that for each of the four impact conditions, the fatigue data for the damaged specimens appear to follow lines of constant K_T. The least severe damage, in terms of an equivalent K_T, appears to be that from the smallest 0.030" (0.76 mm) projectile. These data showed the largest scatter, including several tests indicated by horizontal arrows in Figure 16, where failure in fatigue testing occurred in the grips and not in the gage or leading edge section. In all other tests, the fatigue failure originated at the impact site. In the 0.030" (0.76 mm) impacts, the reproducibility of damage from test to test was the poorest because of the difficulty of hitting the leading edge in the same central location in every test.

To compare damage induced from very small particle impacts with damage from a machined notch of a known geometry, four specimens of the identical geometry were notched with a diamond wire. The notches were made to the same dimensions as those of the craters from the 0.030" (0.76 mm) particles impacted at 1000 ft/s (305 m/s), nominally 0.030" (0.76 mm) across and 0.006" (0.15 mm) deep. These notches produce an elastic stress concentration factor in these specimens of $K_T = 1.7$. The four specimens with the machined notches were fatigue tested in the same manner as the other specimens. The data are presented in Figure 16 and are indicated by the crossed points. It can be noted that the points fell along the same line as a number of the points representing specimens impacted by 0.030" (0.76 mm) particles at 1000 ft/s (305 m/s). Thus, the maximum damage sustained due to the impacts from these small particles in terms of the notch fatigue strength of the material was equivalent to the damage caused by machining similar size damage. For these

22
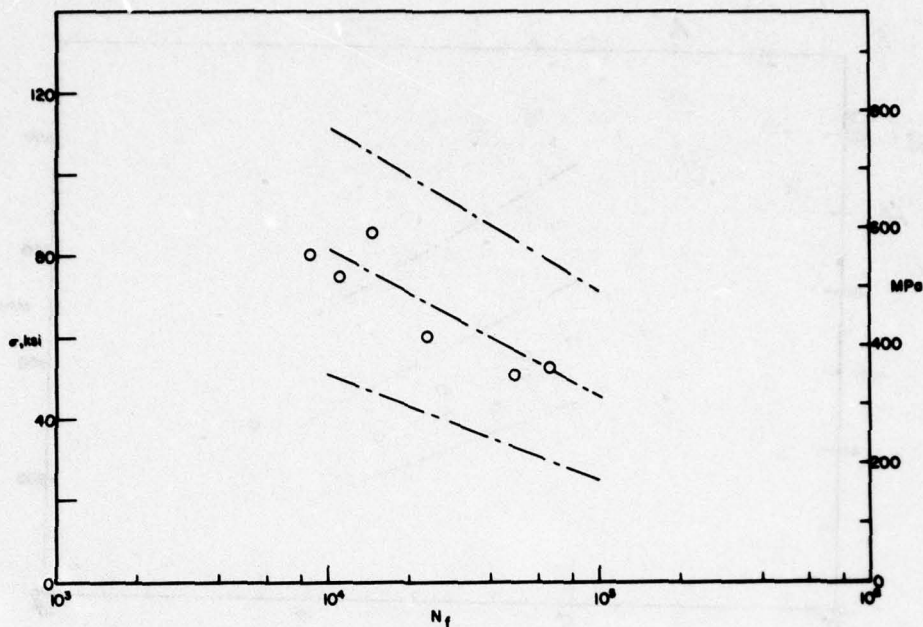
Figure 13. Fatigue data for 0.062" particles, 1600 ft/s.
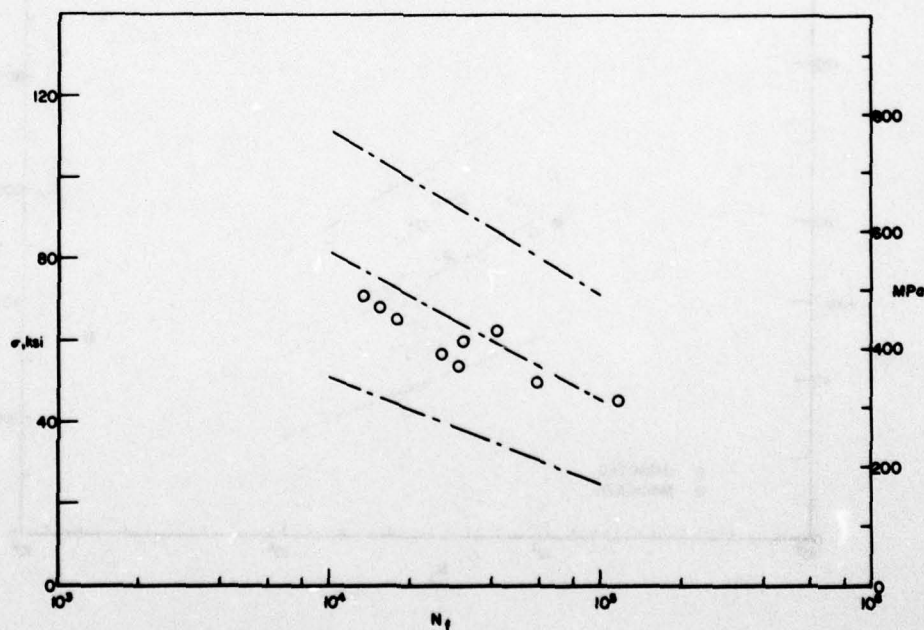
Figure 14. Fatigue data for 0.062" particles, 1100 ft/s.
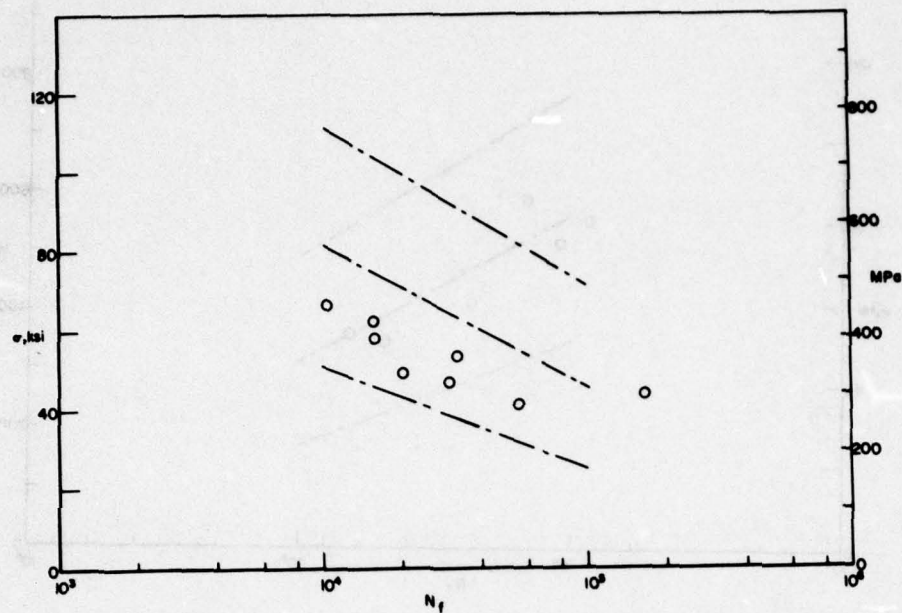
Figure 15. Fatigue data for 0.125" particles, 800 ft/s.
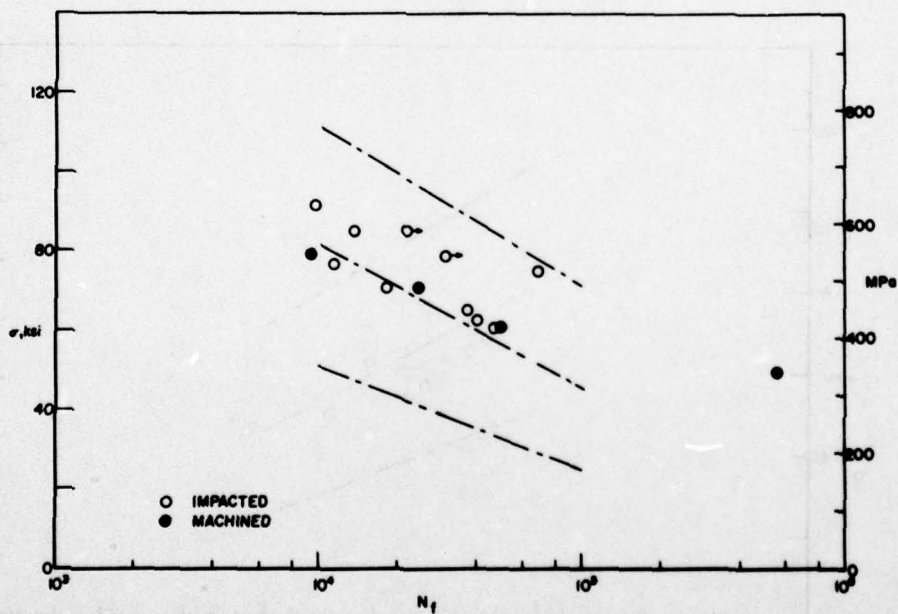
Figure 16. Fatigue data for 0.030" particles, 1000 ft/s.

24

very small nicks it was concluded that the damage sustained
in terms of reduction in fatigue strength is determined more
from the geometry of the crater than from whether the damage
was caused by an impact or machining.

From the point of view of severity of damage in terms of
the notch fatigue strength, the specimens impacted by the
0.062" (1.6 mm) projectiles at both 1600 and 1100 ft/s (490 and
340 m/s) appeared to suffer damage equal to or slightly greater
than those impacted by the smallest 0.030" (0.8 mm) projectiles
at 1000 ft/s (305 m/s). The most severe damage was sustained
due to impacts of 0.125" (3.2 mm) projectiles at 800 ft/s
(240 m/s). The extent of damage can be seen by comparing
Figures 13-16 which all have the three baseline K_T curves.
Note, again, that the stress axis represents average net section
stress in the impacted specimens and does not correct for stress
nonuniformity due to the complex geometry of the leading edge
configuration as described previously.

To further compare the extent of damage in the various
specimens, typical shots were chosen from the four batches of
tests to represent various degrees and sizes of damage. The
six shots chosen are replotted in Figure 17; the photographs
showing the corresponding damage before fatigue testing are
shown in Figure 18. The test conditions are summarized in
Figure 17. Tests 8375, 8368, and 8444 appear to have similar
amounts of damage in terms of fatigue life as can be seen in
Figure 17 by noting the location of those points with respect
to the constant K_T lines. Examination of the photographs in
Figure 18 shows that all three shots have the same type of
damage, namely a semicircle removed from the leading edge. Note
that all three damage sites are geometrically similar, Shot 8375
being approximately one-third the size of the other two. Shots
8433, 8434, and 8432 show apparently increasing damage, respec-
tively, in Figure 17. In Figure 18, it is seen that these three
shots correspond to a bulge, material removal, and a bulge with
a tear, respectively. It is not obvious whether or not there
was any local tearing in Shot 8434. The material removed in

25
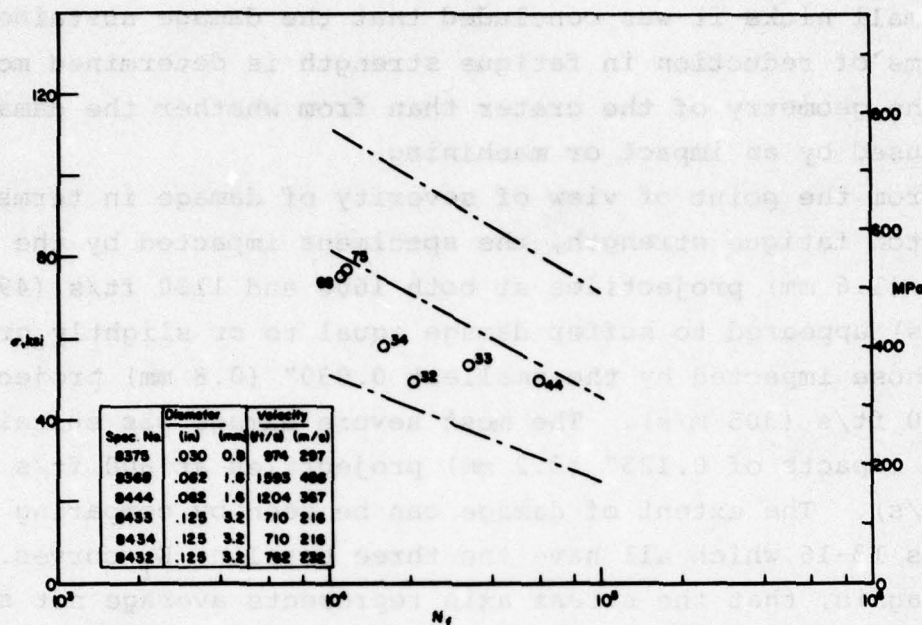
Figure 17. Fatigue data for several shots showing different types of damage.

this shot was, in any case, three times the dimensions of that in Shots 8368 and 8444. Shots 8433, 8434, and 8432 all represent impacts of the largest projectile 0.125" (3.22 mm) at approximately 800 ft/s (240 m/s). Note that the worst case of damage, Shot 8432, represented a situation where the material first bulged and then apprently ripped from the extensive local deformation. The fatigue crack initiated at the rip in this case.

From the results of this series of tests, it was concluded that the extent of damage depended primarily on the type of damage and appeared to be relatively independent of size. The least severe damage for impacted leading edges was a clean perforation with complete material removal. The next worse case was that where the leading edge curled back extensively or bulged. Finally, the worst case was where the curl back or bulge initiated a rip along the leading edge from which the fatigue crack could propagate. For a given projectile size and leading edge geometry, the test data indicated that perforation
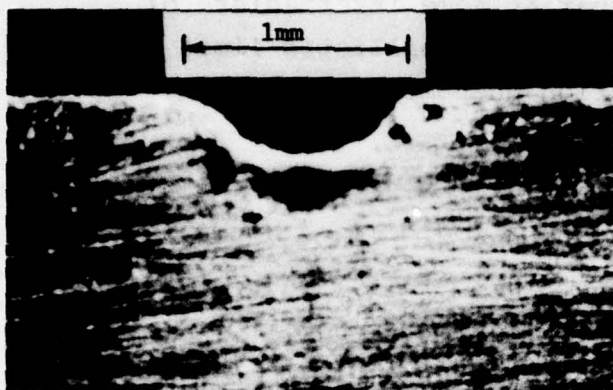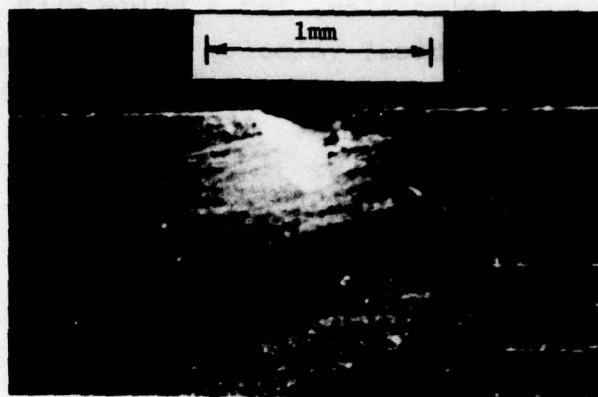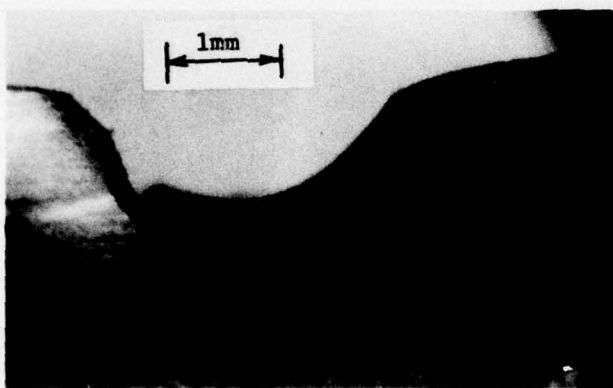
26
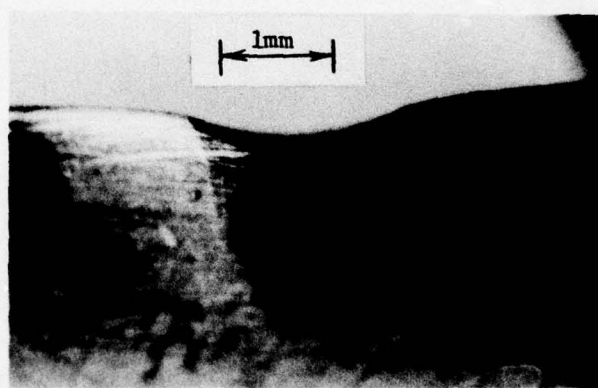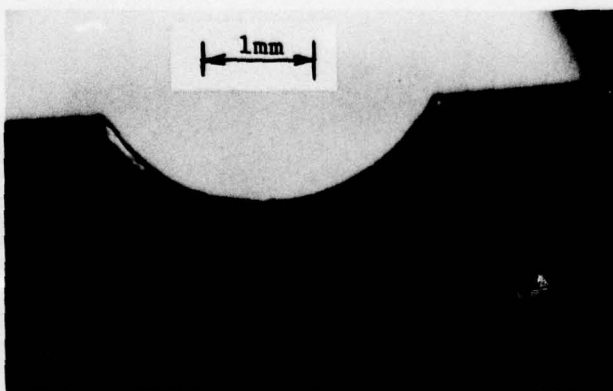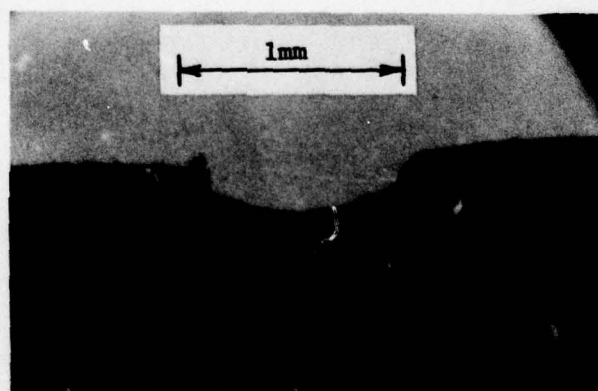
Figure 18. Photographs of several shots showing different types of damage.

occurred at the highest impact velocities, bulging at lower velocities, and a bulge with a tear at some intermediate or critical velocity which is amalogous to a ballistic limit velocity in projectile-plate penetration phenomena.

Figure 18. Photographs of several shots showing different types of damage.

SECTION VI
EFFECT OF PROJECTILE SHAPE, VELOCITY,
AND MATERIAL ON IMPACT DAMAGE

The results of the previous section and observations during earlier tests seemed to indicate that leading edges undergo a range of types of damage as the velocity of the projectile is increased. At very low velocities, the particle bounces off causing no significant damage. As the velocity is increased, the leading edge will be bulged or dented. At higher velocities, the dent or bulge will get larger, eventually tearing or ripping. Finally at even higher velocities, the projectile will perforate, leaving a nick. These observations were based on impacts at an incidence angle of 30°.

A series of impact experiments was conducted using six different projectile sizes and types. These were 0.031" 0.8 mm) chrome spheres, 0.062" (1.6 mm) and 0.125" (3.2 mm) Pyrex spheres, 0.030" (0.8 mm) glass spheres, 0.050"-0.060" (1.3-1.5 mm) silica sand, and 0.020"-0.030" (0.5-0.8 mm) silica sand. Each particle type was fired at a range of velocities from 400 to 1600 ft/s (120 to 490 m/s) against the same leading edge configuration; 8-1-1 Ti sheet material as in the previous tests, an 0.010" (0.25 mm) thick leading edge, a 4° taper and an impact angle of 30°. The specimen was aligned to obtain an on-center impact on the 0.010" (0.25 mm) thick leading edge. A summary of the test conditions is presented in Table 3. Photos of the leading edge damage, looking from the impact side, are presented in Appendix A.

Numerous attempts were made to quantify the damage from all of the tests enumerated above. Although reproducibility of damage was not a problem by itself, the biggest difficulty was to obtain impacts in exactly the same location. For example, a particle 0.030" (0.8 mm) in diameter would miss the leading

edge completely if it drifted by more than 0.020" (0.5 mm) in its flight. Although the accuracy was generally quite good, it was impossible to impact the exact center of the leading edge repeatably, especially with the smaller projectiles. Examination of the photographs will confirm this observation. After a thorough examination of the specimens and the specimen photographs (which included front, rear, and edge view) the shot was chosen for each series which represented, most closely, the condition of impact at the center of the leading edge where tearing appeared. At lower velocities, the specimen was usually dented or bulged. At higher velocities, complete perforation with material removal occurred. The velocity at which tearing combined with a dent or bulge occurred was termed the critical velocity, or velocity causing maximum damage in terms of fatigue strength as discussed in Section V. The critical velocity is plotted as a function of projectile diameter in Figure 19 for the six types of particles. It should be noted that these points represent a best estimate of tearing velocity based on visual observation and are quite subjective. The error band or scatter associated with each point is naturally quite large. Nonetheless, the data appear to demonstrate a definite drop in critical velocity with increasing projectile size for the glass (or Pyrex) spheres. The higher density chrome spheres have a lower critical velocity than the glass spheres for the same size projectile. The silica sand particles also appear to have a lower critical velocity for a given size range than glass. This is probably due to the irregularity of the sand particles.

An attempt was made to study the type and extent of damage sustained on leading edge configurations impacted at a given velocity by particles of various types over a size range from 0.030" to 0.125" (0.8 to 3.2 mm). A nominal velocity of 1000 ft/s (305 m/s) was chosen for this series of experiments. The particles were taken from three groups of debris which were vacuumed from an engine test cell. There was no attempt to identify the type of debris other than by size. It was hypo-thesized that the debris could be scale, weld beads, or other
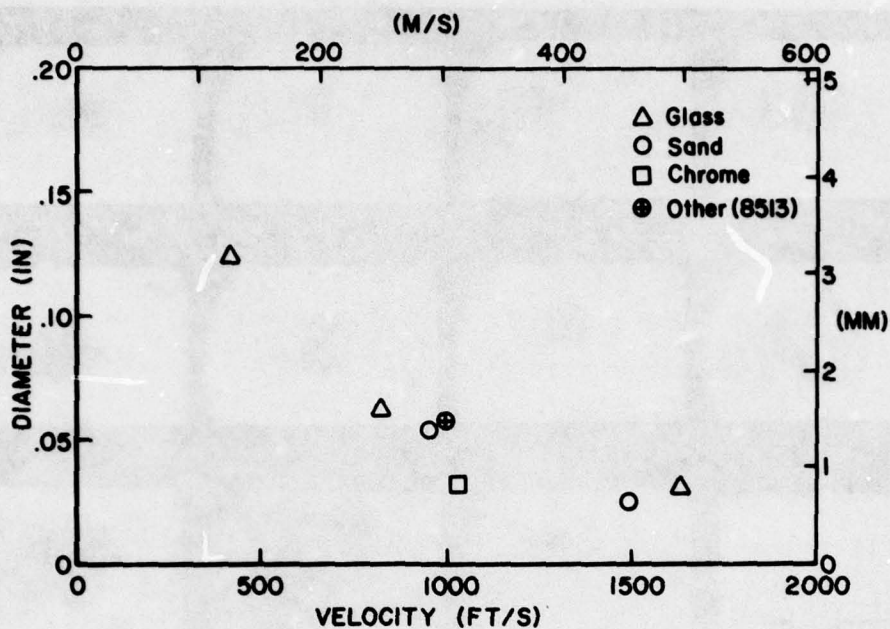
Figure 19. Critical velocity as a function of projectile
diameter (0.010" L.E.).

such matter. From each bag of debris available, a number of
particles were chosen to cover the size range of the debris, not
including small particles, dust, and dirt under 0.030" (0.8 mm).
The particles were photographed and measured and are designated
as Post-Test No. 11, 18, and 23; each particle within the
group being numbered. The particles are shown in Figure 20.
The test data are summarized in Table 4. Photographs of the
damage as seen from the impacted side are presented in Appendix
B.

Examination of the specimens and the photographs from this
series of experiments (Shots 8512-8529) shows the obvious trend
of increasing damage with increased particle size. The large
size particles (0.087" (2.2 mm) Shot 8521, for example, perfor-
ated the leading edge cleanly and removed material at this
(nominal) velocity of 1000 ft/s (305 m/s). Small particles in
the 0.035"-0.040" (0.9-1.0 mm) range (Shots 8512, 8518, 8524)

31
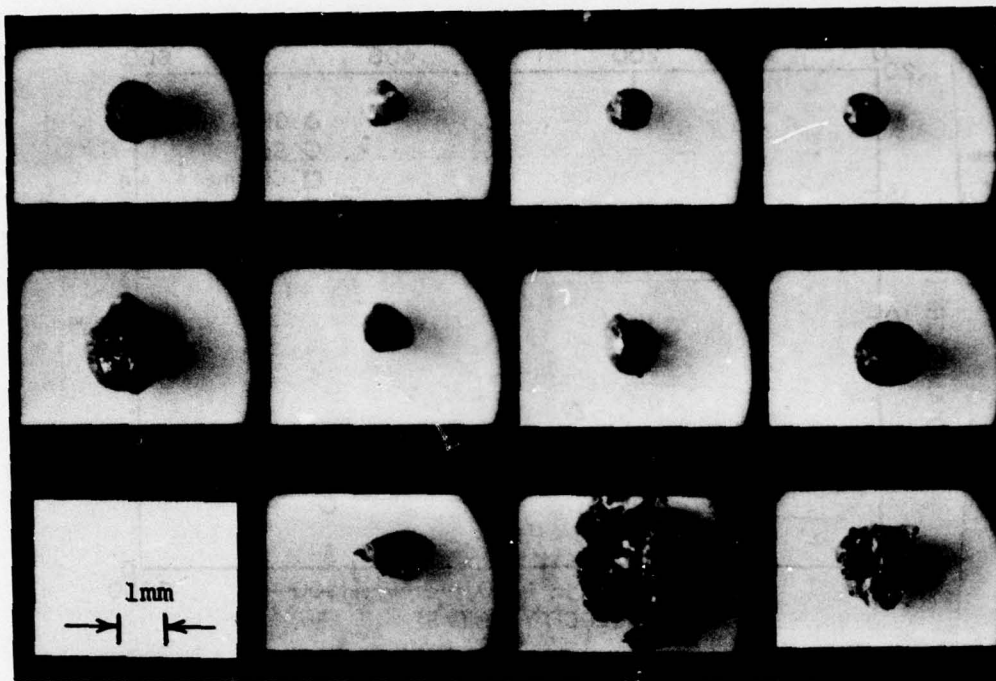
11
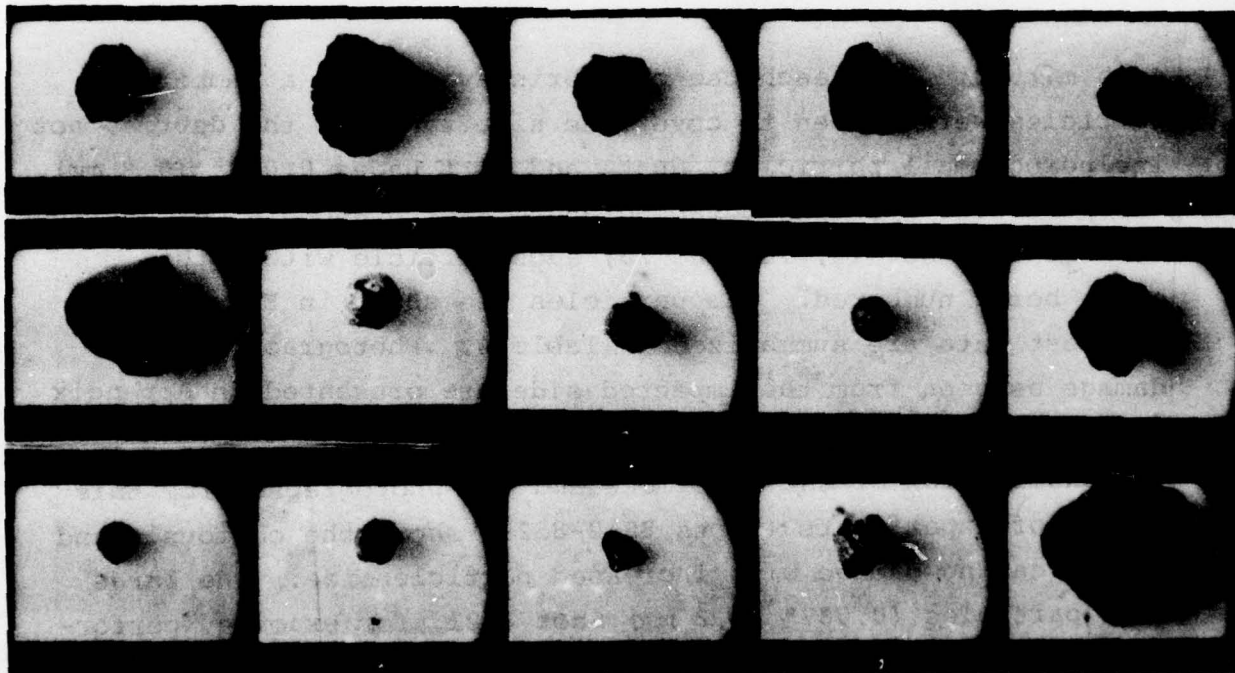
18

Figure 20. Photographs of particles from Post-Test No. 11, 18, and 23 debris.
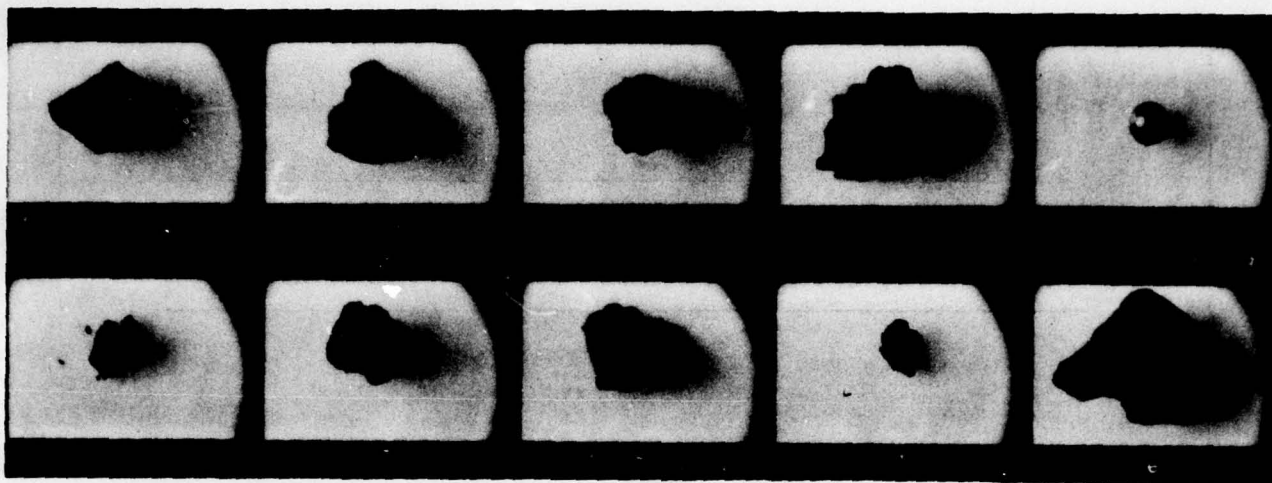
23

Figure 20 (Cont'd). Photographs of particles from Post-Test
No. 11, 18, and 23 debris.

dented the leading edge. One shot, 8513, appeared to cause the
beginning of a tear and could be considered a critical velocity
condition. This shot was plotted in Figure 19 with the previous
data and appeared to follow the established trend, especially
considering the scatter and uncertainty. Based on this series
of tests, it was concluded that a general trend of decreasing
critical velocity with increasing particle size could be esta-
blished and that this trend seemed to be effected somewhat
by geometry (irregularity) and type of material. The biggest
problem in establishing this trend was the ability to impact
leading edges directly on center with these small particles,
although examination of the photographs reveals that the
accuracy was surprisingly good and better than originally
anticipated. Note, again, that all of the above observations
pertained to the case of an 0.010" (0.25 mm) thick leading edge

with a 4° taper angle, and an angle of incidence of the impacting particle with the plane of the blade of 30°.

Figure 20 (Cont'd). Photographs of particles from Post-Test Runs 14, 16, and 21 debris.

SECTION VII
EFFECTS OF LEADING EDGE THICKNESS;
GEOMETRIC SCALING

The last phase of this investigation was to determine the effect of varying leading edge thickness on the type and extent of damage sustained due to particle impacts and to investigate the applicability, if any, of geometric scaling concepts. Geometric scaling is based on the concept of comparing responses of geometrically similar bodies. In this case, we consider spherical projectiles of diameter, d, impacting leading edges of thickness, t. If the ratio of projectile diameter and leading edge thickness is s for two different events, then for a given velocity (the same for both cases) the ratio of momentum or kinetic energy is s^3. It is assumed that the material density is identical in both cases. The force input to the blade or structure has a ratio s^2 and a duration ratio s. The local pressure or stress depends only on the velocity and the areas are related by s^2. (Note that the stress due to one-dimensional impact against a rigid target is ρcv, i.e., depends on the velocity of impact v for a given material having density ρ and wave speed c). The resistance to bending of a structure varies as s^3, s^2 due to the thickness and s for the width or lateral dimension. Resistance to shear or penetration also varies as s^3, s^2 due to the area of a shear plug and s due to the thickness. With identical stresses in both cases, the deflections should scale linearly with ratio s. The two events, then, should be identical as long as wave propagation and resulting inertia effects are not important. One can expect, for example, that the damage in an 0.010" (0.25 mm) thick specimen due to an impact of an 0.062" (1.6 mm) projectile would be geometrically similar to that in an 0.020" (0.51 mm) thick specimen impacted with an 0.125" (3.2 mm) projectile.

35

A series of tests was performed involving impacts of glass
and steel spheres against leading edge thicknesses of 0.015",
0.020", and 0.030" (0.38, 0.51, and 0.76 mm). Recall that all
previous tests were made on 0.010" (0.25 mm) thicknesses. As
before, the incidence angle was 30° and the blade taper was 4°.
The material for all but the 0.030" (0.8 mm) thick blades was
from the same sheet of 8-1-1 Ti. For the 0.030" (0.8 mm) thick
blades (Shots 8602-8606) a piece of 0.125" (3.2 mm) thick sheet
of Ti 6Al-4V was used. This grade of titanium is similar to
8-1-1 Ti in mechanical properties. Although it has a slightly
lower modulus of elasticity, it was felt it would give similar
results to 8-1-1 Ti. The thicker sheet was believed necessary
for the specimen blank because of the large thickness of the
leading edge, 0.030" (0.8 mm) and the large size of the projec-
tile 0.250" (6.4 mm) which was felt would cause damage over an
extensive area. The test series covered projectile sizes of
0.062", 0.125", and 0.250" (1.6, 3.2 and 6t4 mm) diameter and
impact velocities from approximately 400 to 1600 ft/s (120 to
490 m/s). The test conditions are summarized in Table 5. It
was originally planned to use Pyrex (glass) projectiles for this
entire series of tests. However, it was discovered that in
shooting at high velocities against thicker leading edges, the
glass projectiles were breaking up upon impact. In all previous
tests, the projectile had remained essentially intact upon
impact. Thus, a switch was made to steel projectiles for all
subsequent shots, with the exception of a few shots at lower
velocities, to avoid the uncertainty surrounding the effect of
projectile break-up upon the damage inflicted on the blades.

To investigate the concept of geometric scaling, the pro-
cedure described in the previous section was followed. To
identify the critical velocity of impact, all of the impacted
test specimens were examined visually and through magnified
photos to identify those having damage typical of that encoun-
tered at critical velocity, defined previously as the velocity
which caused bulging and incipient tearing. Again, this

36

identification of specimens was subjective. Figure 21 shows
rear side photos of the seven specimens selected as well as
previous shot 8513 on an 0.010" (0.25 mm) thick specimen.
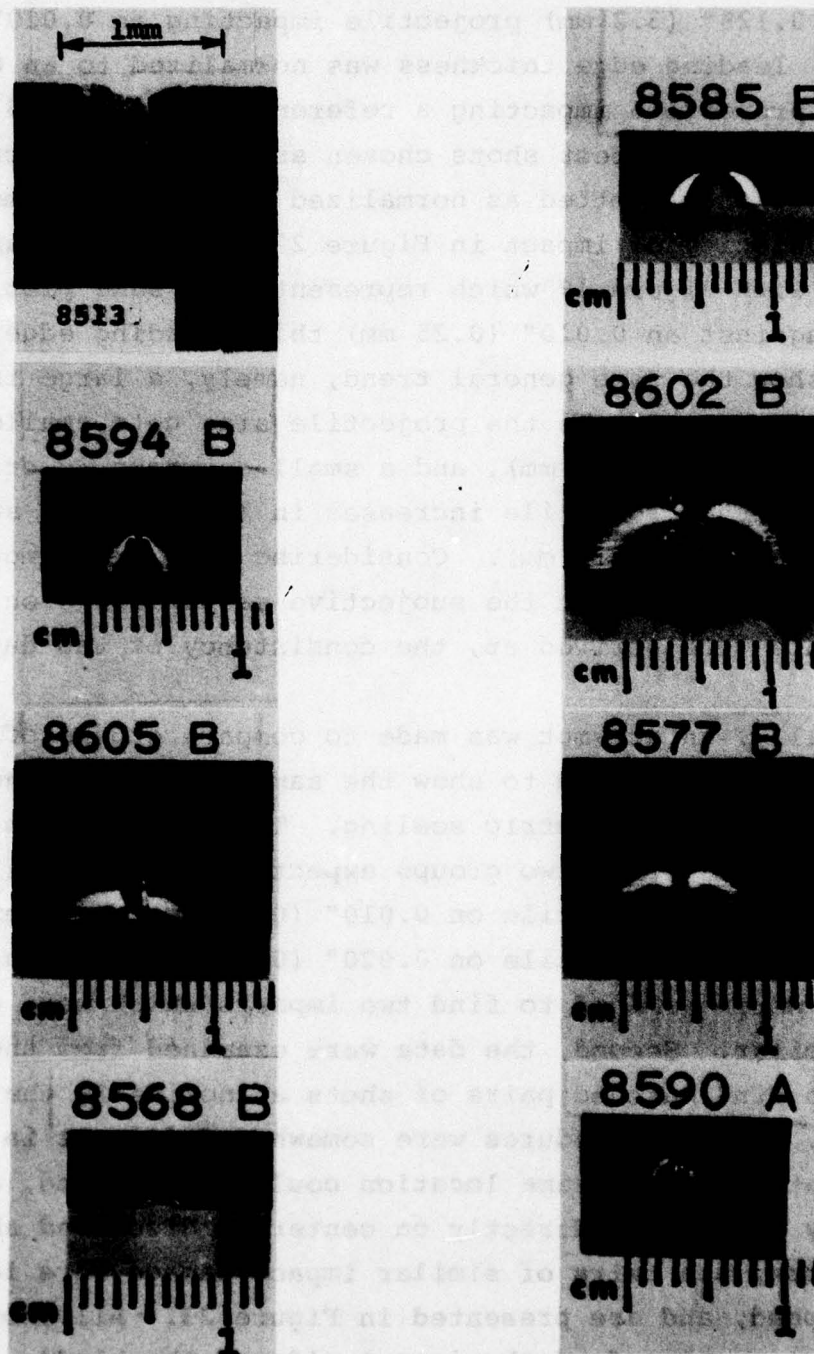
Figure 21. Photographs of typical leading edge damage as seen
from rear side.

The projectile size for each of the critical damage speci-
men shots chosen was normalized to that causing equivalent
damage in an 0.010" (0.25 mm) thick leading edge specimen
following the concept of geometric scaling outlined above.
Thus, an 0.125" (3.2 mm) projectile impacting an 0.020"
(0.51 mm) leading edge thickness was normalized to an 0.062"
(1.6 mm) projectile impacting a reference 0.010" (0.25 mm)
leading edge. The test shots chosen as representing critical
damage were then plotted as normalized projectile diameter
against velocity of impact in Figure 22. Figure 22 can be
compared with Figure 19 which represents the same plot for the
impacts against an 0.010" (0.25 mm) thick leading edge. Both
figures show the same general trend, namely, a large increase
in critical velocity as the projectile size gets smaller than
approximately 0.04" (1 mm), and a small decrease in critical
velocity as the projectile increases in (normalized) size above
approximately 0.08" (2 mm). Considering the large amount of
scatter in the data and the subjective manner in which these
data points were arrived at, the consistency of the data is
good.

Finally, an attempt was made to compare groups of shots
which might be expected to show the same type of damage based
on the concept of geometric scaling. This was done in two ways.
First, specimens from two groups expected to show similar damage
0.062" (1.6 mm) projectile on 0.010" (0.25 mm) specimen and
0.125" (3.2 mm) projectile on 0.020" (0.5 mm) specimen, for
example, were examined to find two impacts which were geometri-
cally similar. Second, the data were examined from the two
groups to find matched pairs of shots at nominally the same
velocity. These procedures were somewhat difficult in that only
impacts at the exact same location could be compared, and not
that many shots were directly on center as discussed above.
Nonetheless, six pairs of similar impact damage were identified,
photographed, and are presented in Figure 23. All photos show
the damage as seen from the impact side of the blade. The
interpretation of these photos is presented below.

38
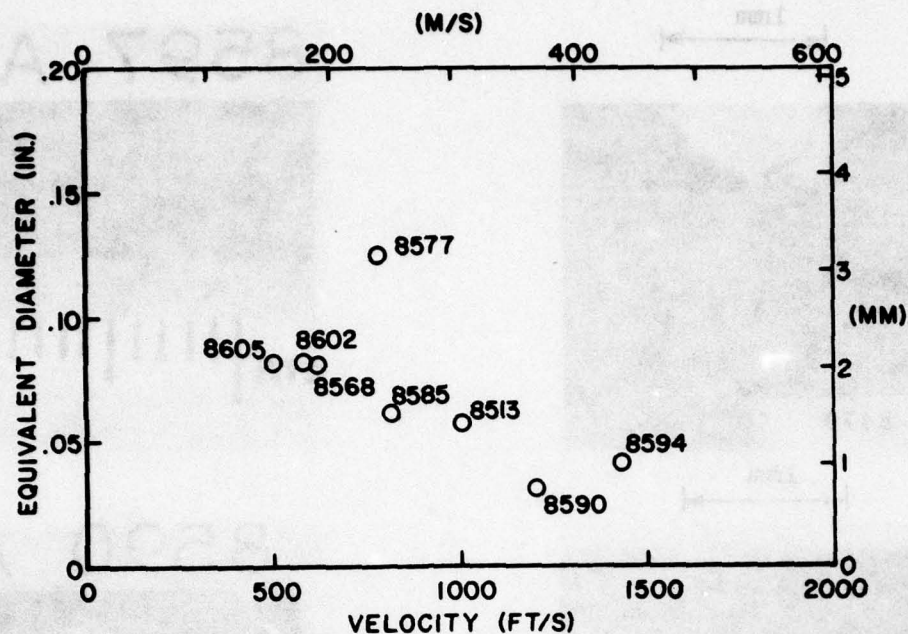
Figure 22. Critical velocity for impacts against thicker
leading edges; plotted as equivalent diameter
for 0.010" L.E.

To illustrate certain features of the damage, and for
reference purposes, the data of Figures 19 and 22 were replotted
in Figure 24. The open triangles represent the points from
shots on 0.010" (0.25 mm) thick leading edges. The solid
triangles represent the points from shots on thicker leading
edge configurations, the projectile diameter being normalized as
explained above. The remaining points are identified individ-
ually and are not, in general, meant to represent the critical
velocity. They are plotted to illustrate their location with
respect to the critical velocity curve as explained in detail
below. Several points are shown with two symbols, one repre-
senting a critical velocity point to establish the curve and the
second symbol to identify the point for discussion purposes.

Shots 8479 and 8597, Figure 23a, are examples of perfora-
tion where material removal has occurred. These two points,
plotted in Figure 24, come out to the right or along the curve
or scatter band representing the critical velocity points. Both
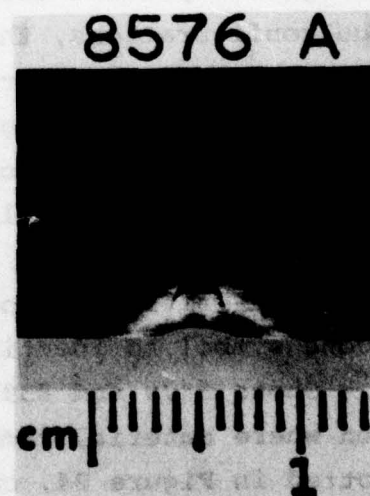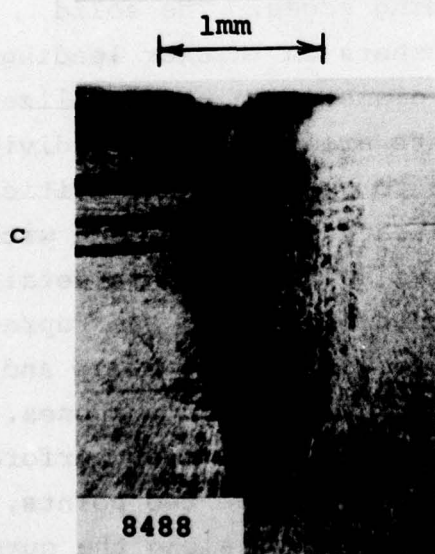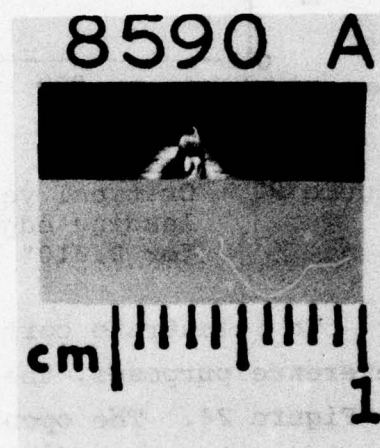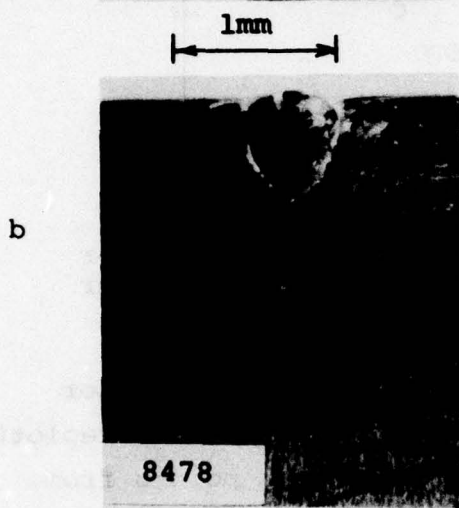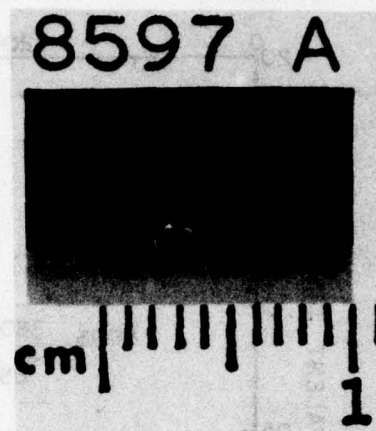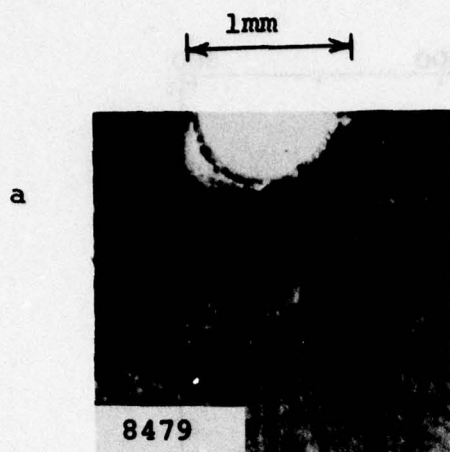
Photographs of pairs of specimens showing similar damage.
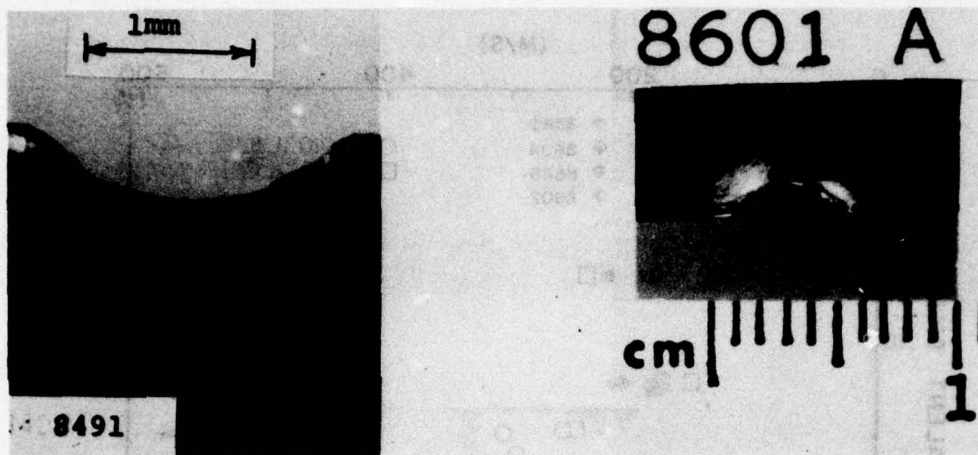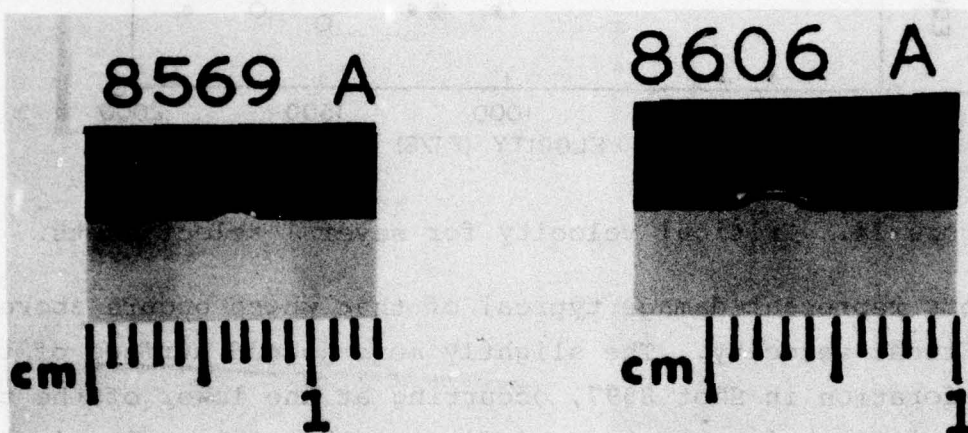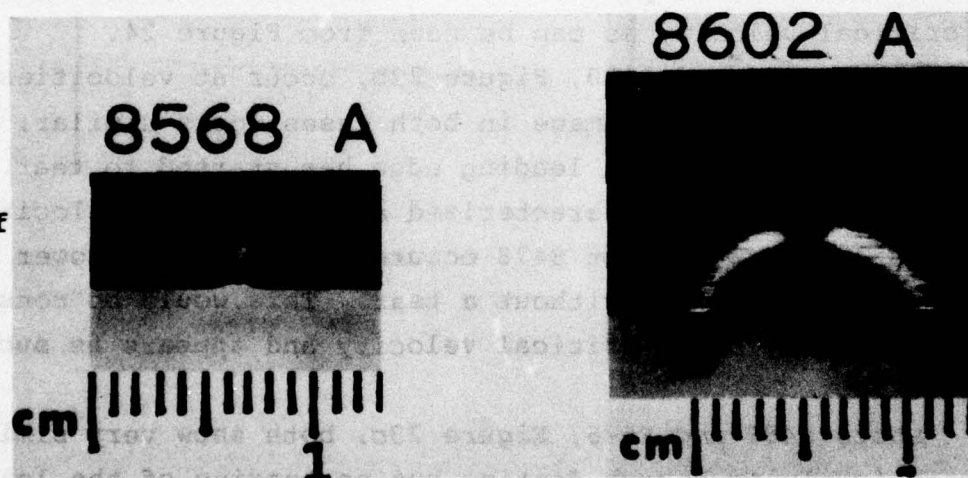
Photographs of pairs of specimens showing
similar damage.
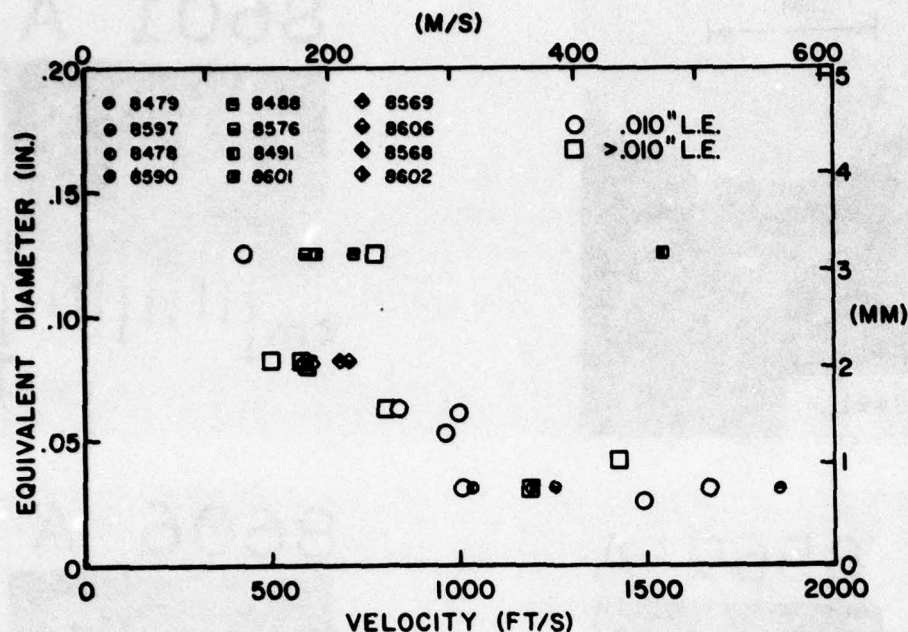
Figure 24. Critical velocity for several select shots.

shots represent damage typical of that which occurs above the critical velocity. The slightly more jagged surface of the perforation in Shot 8597, occurring at the lower of the two velocities being compared, indicates that this point is close to critical velocity as can be seen from Figure 24.

Shots 8478 and 8590, Figure 23b, occur at velocities close to one another. The damage in both cases looks similar, although in Shot 8590 the leading edge has started to tear. This was one of the shots characterized as at critical velocity, in Figures 22 and 24. Shot 8478 occurs at a slightly lower velocity and shows a dent without a tear. This would be considered to be slightly below critical velocity and appears as such in Figure 24.

Shots 8488 and 8576, Figure 23c, both show very similar damage involving severe denting but no tearing of the leading edge. The velocities of these shots are close to one another and are considered to be slightly below critical. These points, plotted in Figure 24, fall within or to the left of the scatter

42

band. Although no tearing of the leading edge occurred, it is felt that these were close to critical velocity because of the extensive bulging and the plot of Figure 24 appears to support this premise.

Shots 8491 and 8601, Figure 23d, are a pair of shots showing very similar damage in the form of complete perforation with material removal. These points would both be expected to fall above the critical velocity. Note, however, the great difference in velocities. Although, as expected, Shot 8491 is well to the right of the critical velocity scatter band in Figure 24, Shot 8601 falls within the band. Shot 8601 is a good example of the variability in damage which can be expected and the difficulty in determining the critical velocity with a great deal of accuracy from a limited number of shots.

Shots 8569 and 8606, Figure 23e, occurred at almost identical velocities and look very similar in type of damage. Both show a crater, indicating complete perforation, although both have rather jagged features along the crater. This indicates that the critical velocity has just been exceeded. The plot of Figure 24 appears to verify this information, the two points falling within or slightly to the right of the critical velocity band.

Shots 8568 and 8602, Figure 23f, were chosen as representative of damage occurring at the critical velocity. Both show an extensive bulge with a slight tear on the leading edge. Both occurred at almost the same velocity and plot within the critical velocity scatter band. This example illustrates the concept of geometric scaling quite well since the two shots were made on leading edge thicknesses of 0.015" and 0.030" (0.38 and 0.76 mm) with projectiles of 0.125" and 0.250" (3.2 and 6.4 mm) diameter, respectively, and also appear to be consistent with baseline data generated on .010" (0.25 mm) thick leading edges.

43

SECTION VIII
SUMMARY AND CONCLUSIONS

Leading edge impact damage was studied by performing a series of hard particle impact tests on titanium and visually observing the damage. Fatigue tests were used as a measure of damage and to investigate the applicability of the concept of an equivalent elastic stress concentration factor to characterize severity of damage. Geometric scaling was examined by using different leading edge thicknesses and various projectile sizes. Finally, the concept of a critical velocity to quantitatively evaluate damage was investigated.

Although several conclusions can be drawn from this investigation, it must first be pointed out that this investigation was in no way comprehensive and was not expected to provide a detailed analysis of hard particle leading edge impact damage. It was also not intended to reproduce damage in any particular engine blade or material. Rather, it was intended to investigate some of the primary features of impact damage and to delineate the more important variables and parameters involved in hard particle impact phenomena.

The feasibility of evaluating leading edge damage from small hard particle impacts was established early in the investigation. It was demonstrated that single particle impacts using glass, steel, or sand having diameters as small as 0.030" (0.8 mm) could be achieved, fairly reproducibly, against 0.010" ().25 mm) thick leading edges over a velocity range from approximately 600 to 1600 ft/s (180 to 490 m/s).

Small particles of sand or glass, having diameters as small as 0.030" (0.8 mm), do cause damage to 0.010" (0.25 mm) thick leading edges in titanium and have a detrimental effect on the fatigue strength of the material (or blade). The extent of damage from a range of particle sizes was evaluated quantitatively by performing a series of fatigue tests at various load

44

levels on specimens impacted under nominally identical conditions. The data demonstrated reasonable reproducibility and showed that the extent of a particular type of damage could be categorized in terms of an equivalent elastic stress concentration factor. Because of the complex geometry of the fatigue specimen and the resulting non-uniform stress state, the exact concentration factors were not determined. It is suggested that this fatigue testing procedure could be utilized to obtain quantitative fatigue data in terms of S-N curves for impact damaged specimens if a new fatigue specimen were designed having a uniform stress state while maintaining the leading edge geometry at the region of impact. An additional piece of information obtained from the fatigue tests was that the damage sustained from very small particles,which perforated the leading edge completely and removed material, was essentially the same as that caused by machining a notch of the same geometry in terms of fatigue strength. The fatigue tests also indicated that different degrees of damage occurred depending on impact velocity. For a given particle impacting a given leading edge, a progression of damage types appeared as velocity increased. Up to a certain velocity, essentially no damage occurred, the particle apparently bouncing off the blade. As the impact velocity was increased, increasing amounts of denting or bulging of the leading edge occurred. At some high velocity, designated the critical velocity, the dent or bulge was of maximum size and the leading edge began to tear or rip. At higher velocities, the projectile completely perforated the blade leaving increasingly smooth holes as velocity increased. The fatigue tests indicated that the maximum damage, or the greatest reduction in fatigue life, occurred at the critical velocity when the blade had been dented and a tear was formed. The damage at this point was referred to as critical damage. In terms of fatigue strength, the severe bulge was the next most severe condition. Perforations with smooth surfaces, obtained at velocities much higher than the critical velocity, and small dents, appeared to be the least severe type of damage experienced.

45

Thus, damage does not monotonically increase with impact velocity but follows, instead, the trend found in classical ballistic perforation phenomena.

The effects of projectile material, impact angle, and blade temperature were all examined very briefly. Within the very narrow range of parameters investigated, the change in damage as a function of these variables was minor or non-existent. It was discovered later in the testing that glass spheres shattered upon impact with thick leading edges at high velocities. The experimental data obtained from impacts when the projectile shattered were not used in arriving at any of the conclusions in this study. The results here are applicable exclusively to impact conditions where the impacting projectile remains essentially intact.

The concept of geometric scaling was investigated by performing a series of tests using different leading edge thicknesses and different projectile sizes. Observation of the type of damage, and plots of critical velocity versus particle size (in relation to leading edge thickness) appeared to validate the scaling concepts. Considering the amount of scatter in the results and the subjective manner in which damage was evaluated, the scaling law seemed to work quite well over the ranges investigated.

Finally, it can be concluded that a methodology has been developed and demonstrated for evaluating the effects of hard particle impacts on compressor blades in jet engines. It would appear that the vulnerability of a specific blade to small hard particles ingested into an engine could be established through laboratory tests on the given leading edge configuration. The testing of a full-scale engine or a stage of blades does not appear to be necessary if single particle can be impacted against stationary blades as demonstrated in this program. This type of simulation, combined with fatigue or static testing under stress conditions representative of actual conditions in the blade, can be used to quantitatively evaluate structural degradation from small hard particle F.O.D.

46
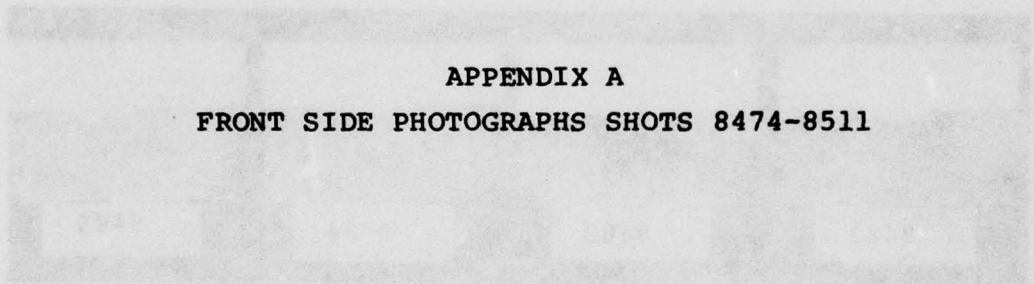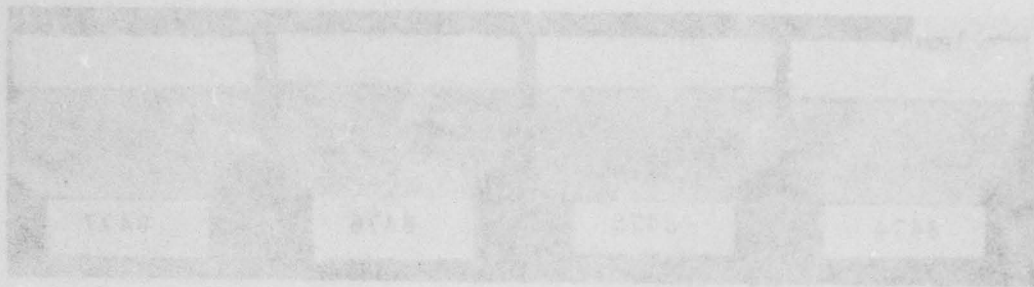
APPENDIX A

FRONT SIDE PHOTOGRAPHS SHOTS 8474-8511

47

48
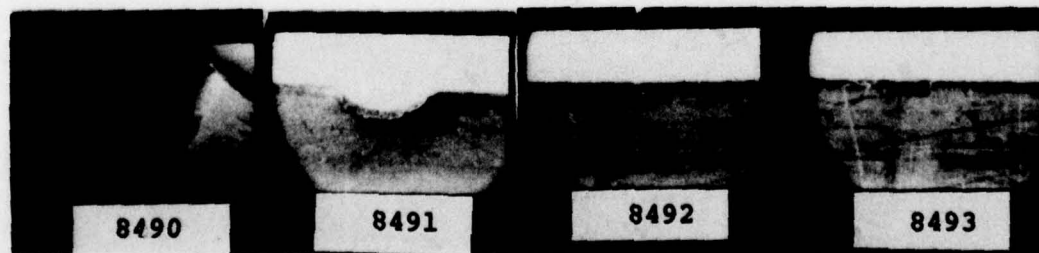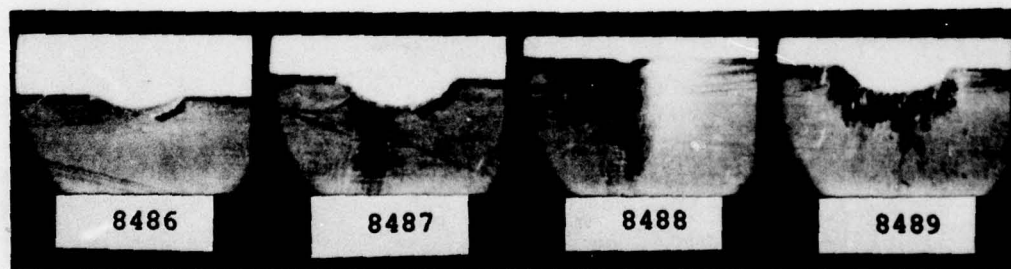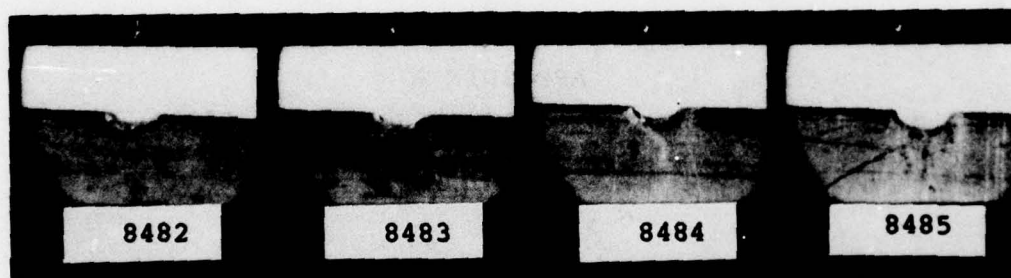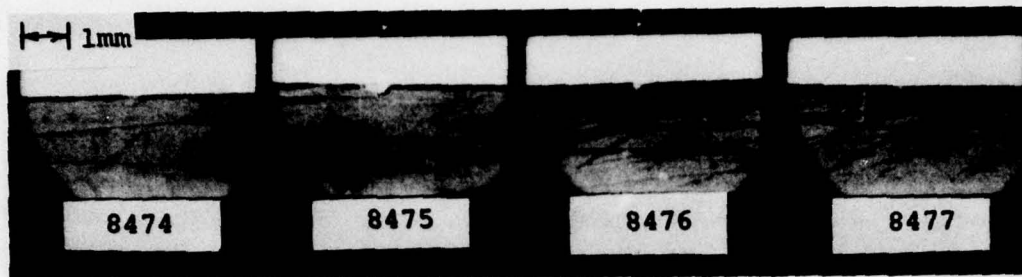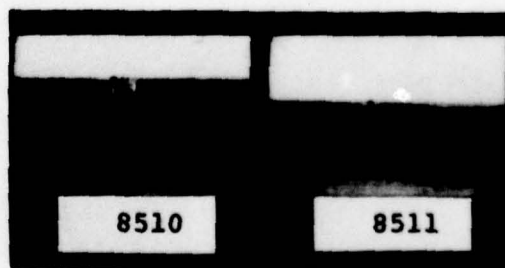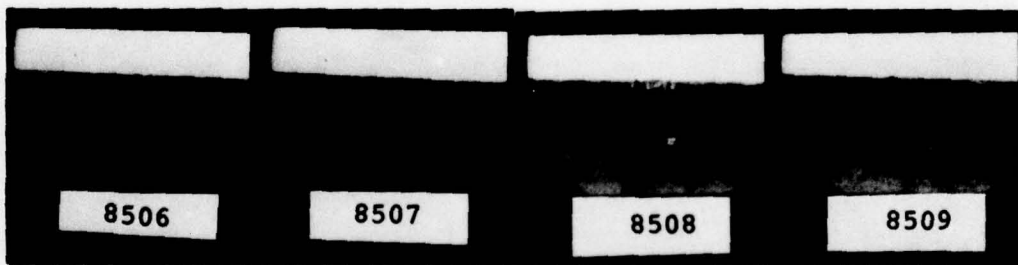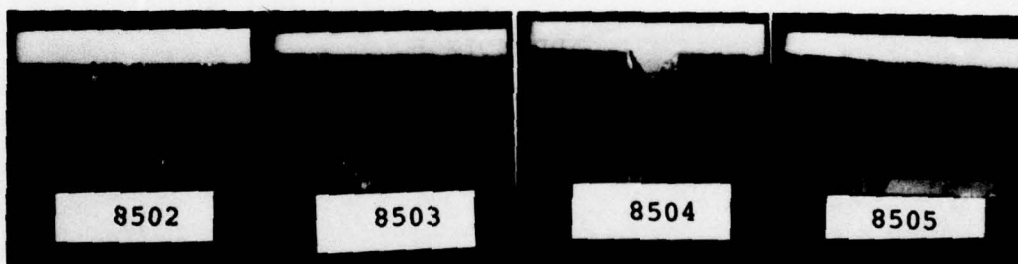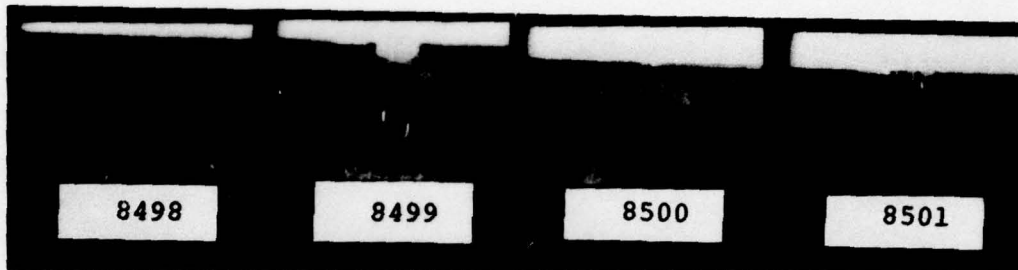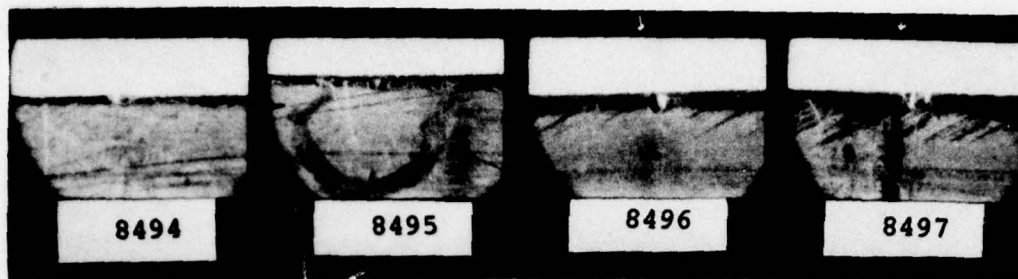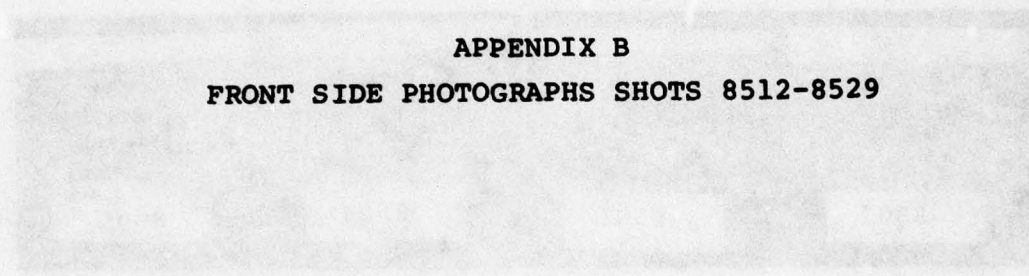
APPENDIX B
FRONT SIDE PHOTOGRAPHS SHOTS 8512-8529

8512   8513   8514   8515

8516   8517   8518   8519

8520   8521   8522   8523

8524   8525   8526   8527

⊢→1mm

8528   8529

51
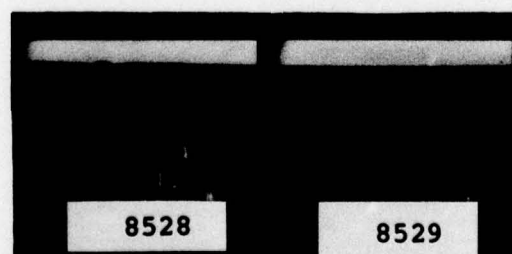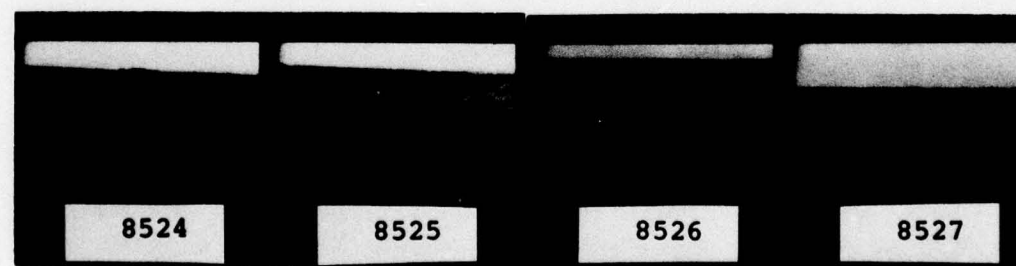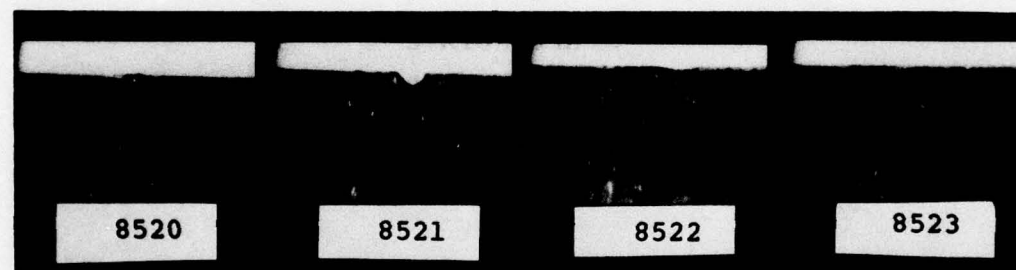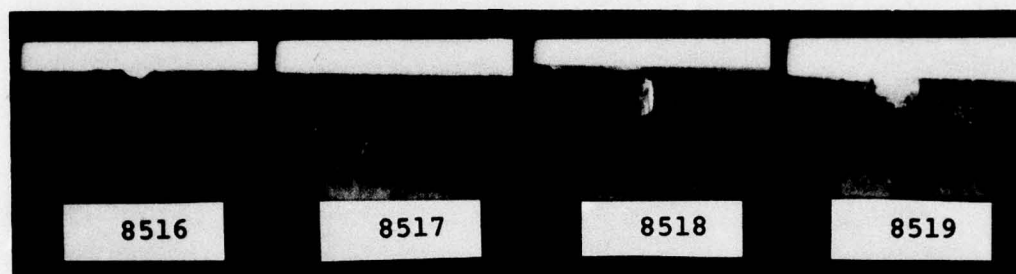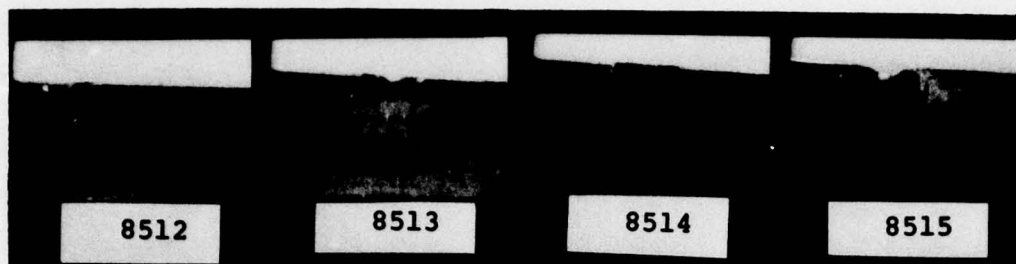
APPENDIX C
TABLES OF TEST CONDITIONS

TABLE 1. SUMMARY OF TEST CONDITIONS FOR PRELIMINARY SHOTS AND FIRST SERIES Of LEADING EDGE IMPACTS

Shot No.	Target Material	Target Thickness At Point Of Impact (mm)	Target Support Method	Projectile Type	Projectile Size (mm)	Impact Velocity (m/s)	Type of Impact	Remarks
8299	Ti 6Al-4V	1.32	Cantilever	Glass Beads	0.50 to 0.59	316.2	90° in-center	Multiple impacts which generated a peened surface over a 5.1mm diameter area.
8300	Ti 75	0.51	Cantilever	Glass Beads	0.50 to 0.59	319.2	45° on edge	Multiple impacts which generated a peened surface.
8301	Ti 6Al-4V	1.32	Cantilever	Irregular Shaped Glass	0.50 to 0.59	316.2	90° in center	Multiple impacts over an area 3.8mm in diameter
8302	Ti 6AL4V	1.32	Cantilever	Pyrex Beads	1.59	314.6	90° in center	4 impacts over an area 3.8mm in diameter
8303	Ti 6AL4V	1.32	Cantilever	Irregular Shaped Mgo	0.84 to 1.19	316.2	90° in center	Multiple impacts over an area 3.8mm in diameter
8304	Ti 6AL4V	1.32	Cantilever	Glass Beads	0.18 to 0.25	317.9	90° in center	Multiple impacts which generated a peened surface over an area 5.1mm in diameter
8305	Ti 6AL4V	1.32	Cantilever	Silica Sand	0.50 to 0.59	307.5	90° in center	Multiple impacts which generated a pitted surface over an area 5.1mm in diameter with 2 stray impacts 5.1mm away
8306	Ti 6AL4V	1.32	Cantilever	Ottowa Sand	0.50 to 0.59	311.8	90° in center	Multiple impacts which generated a pitted surface over an area 3.8mm in diameter
8307	Ti 8-1-1	1.60	Cantilever	Glass Beads	0.50 to 0.59	312.7	90° in center	Multiple impacts which generated a peened surface over an area 3.8mm in diameter
8308	Ti 8-1-1 (taper ground)	1.60	Cantilever	Pyrex Beads	1.59	330.4	90° in center	4 impacts over an area 3.0mm in diameter
8309	Ti 8-1-1	0.25	Cantilever	Glass Beads	0.50 to 0.59	314.2	30° in center	Multiple impacts which generated a peened edge and permanent deformation of 0.2mm
8310	Ti 8-1-1	0.25	Cantilever	Silica Sand	0.25 to 0.30	317.0	30° on edge	Multiple impacts which generated a peened surface.

53

TABLE 1. SUMMARY OF TEST CONDITIONS FOR PRELIMINARY SHOTS
AND FIRST SERIES OF LEADING EDGE IMPACTS (CONT'D)

Shot No.	Target Material	Target Thickness At Point Of Impact (mm)	Target Support Method	Projectile Type	Projectile Size (mm)	Impact Velocity (m/s)	Type of Impact	Remarks
8311	Ti 8-1-1	0.25	Cantilever	Silica Sand	0.50 to 0.59	304.5	30° on edge	Multiple impacts which generated a pitted edge and permanent deformation of .2mm also some material loss
8312	Ti 8-1-1	0.25	Cantilever	Silica Sand	0.84 to 1.0	311.2	30° on edge	Multiple impacts which generated a pitted edge with some loss of material and permanent deformation of 0.5mm
8313	Ti 8-1-1	0.25	Cantilever	Silica Sand	0.50 to 0.59	317.9	30° on edge	Multiple impacts which generated a pitted edge with some loss of material and permanent deformation of 0.1mm
8314	Ti 8-1-1	0.25	Cantilever	Silica Sand	0.84 to 1.0	309.4	30° on edge	Sand grains stayed in a tight pattern behaving as a single impact. Roll back and splitting also permanent deformation of 1.4mm
8315	Ti 8-1-1	0.25	Cantilever	Glass Beads	0.50 to 0.59	316.1	30° on edge	Multiple impacts which generated a peened edge and permanent deformation of .4mm
8316	Ti 8-1-1	0.25	Cantilever	Glass Beads	0.25 to 0.30	312.7	30° on edge	Multiple impacts which generated a peened surface.
8317	Ti 8-1-1	0.25	Cantilever	Pyrex Beads	1.59	310.9	30° on edge	6 impacts with 2 on edge, some loss of material and permanent deformation of 0.5mm
8318	Ti 8-1-1	0.25	Cantilever	Pyrex Beads	1.59	312.1	30° on edge	3 impacts with 2 on edge, some loss of material and permanent deformation of 0.5mm
8319	Ti 8-1-1	0.25	Cantilever	Silica Sand	0.50 to 0.59	294.7	30° on edge	Sand Grains stayed in a close group behaving as a single impact. Roll back and permanent deformation of 0.7mm

54

TABLE 1. SUMMARY OF TEST CONDITIONS FOR PRELIMINARY SHOTS AND FIRST SERIES OF LEADING EDGE IMPACTS (CONT'D)

Shot No.	Target Material	Target Thickness At Point Of Impact (mm)	Target Support Method	Projectile Type	Projectile Size (mm)	Impact Velocity (m/s)	Type of Impact	Remarks
8320	Ti 8-1-1	0.25	Cantilever	Silica Sand	0.50 to 0.59	501.1	30° on edge	Sand grains stayed closely grouped. Roll back and splitting, some material loss and permanent deformation of 1.1mm
8321	Ti 8-1-1	0.18	Cantilever	Silica Sand	0.50 to 0.59	519.1	30° on edge	Multiple impacts which generated a pitted edge with splitting and material loss. Also roll back and permanent deformation of 1.0mm
8322	Ti 8-1-1	0.25	Cantilever	Silica Sand	1.00 to 1.19	310.3	30° on edge	Multiple impacts which generated a pitted edge with roll back and permanent deformation of 0.4mm
8323	Ti 8-1-1	0.25	Cantilever	Silica Sand	1.00 to 1.19	306.0	30° on edge	3 impacts on edge. Some material loss and permanent deformation of 0.3mm
8324	Ti 8-1-1	0.25	Cantilever	Glass Beads	0.15	304.8 est.	30° on edge	Multiple impacts which were visible only with 1x magnifier.
8325	Ti 8-1-1	0.25	Cantilever	Glass beads	0.15	315.2	30° on edge	Multiple impacts which were visible only with 1x magnifier
8326	Ti 8-1-1	0.23	Cantilever	Silica Sand	0.50 to 0.59	487.7	30° on edge	Multiple impacts with 4 on edge which generated a pitted edge with some material loss and permanent deformation of 0.3mm
8327	Ti 8-1-1	0.23	Cantilever	Silica Sand	0.50 to 0.59	450.2	30° on edge	Multiple impacts with 5 on edge which generated a pitted edge with some material loss and permanent deformation of 0.3mm
8328	Ti 8-1-1	0.23	Cantilever	Silica Sand	1.00 to 1.19	479.8	30° on edge	Multiple impacts with 6 on edge which generated a pitted edge with some material loss and permanent deformation of 0.3mm

55

TABLE 1. SUMMARY OF TEST CONDITIONS FOR PRELIMINARY SHOTS AND FIRST SERIES OF LEADING EDGE IMPACTS (CONT'D)

Shot No.	Target Material	Target Thickness At Point Of Impact (mm)	Target Support Method	Projectile Type	Projectile Size (mm)	Impact Velocity (m/s)	Type of Impact	Remarks
8340	Ti 8-1-1	0.23	Cantilever	Glass Beads	0.15	511.1	30° on edge	Multiple impact which generated a peened edge
8341	Ti 8-1-1	0.23	Cantilever	Glass Beads	0.15	511.1	30° on edge	Multiple impact which generated a peened edge with permanent deformation of 0.2mm
8342	Ti 8-1-1	0.23	Cantilever	Glass Beads	0.15	465.4	30° on edge	Multiple impacts which generated a peened edge
8343	Ti 8-1-1	0.25	Cantilever	Glass Beads	0.50 to 0.59	310.6	10° on edge	Multiple impacts which generated a peened edge and permanent deformation of 0.1mm
8344	Ti 8-1-1	0.25	Cantilever	Glass Beads	0.50 to 0.59	487.7	10° on edge	Multiple impacts which generated a peened edge with loss of material and permanent deformation of 0.3mm
8345	Ti 8-1-1	0.25	Cantilever	Silica Sand	0.50 to 0.59	481.0	10° on edge	Multiple impacts which generated a pitted edge with material loss and permanent deformation of 0.2mm
8346	Ti 8-1-1	0.25	Cantilever	Silica Sand	0.50 to 0.59	303.6	10° on edge	Multiple impacts which generated a pitted edge with material loss and permanent deformation of 0.2mm
8347	Ti 8-1-1	0.20	Cantilever	Glass Beads	0.50 to 0.59	316.1	30° on edge at 250°F	Multiple impacts with 4 on edge which generated permanent deformation of 0.1mm
8348	Ti 8-1-1	0.20	Cantilever	Glass Beads	0.50 to 0.59	439.2	30° on edge at 250°F	Multiple impacts which generated a peened edge with some roll back and splitting also permanent deformation of 0.5mm
8349	Ti 8-1-1	0.20	Cantilever	Silica Sand	0.50 to 0.59	459.0	30° on edge at 250°F	Multiple impacts which generated a pitted edge with material loss and permanent deformation of 0.4mm
8350	Ti 8-1-1	0.20	Cantilever	Silica Sand	0.50 to 0.59	310.6	30° on edge at 250°F	Multiple impacts which generated a pitted edge with material loss and permanent deformation of 0.3mm

TABLE 1. SUMMARY OF TEST CONDITIONS FOR PRELIMINARY SHOTS
AND FIRST SERIES OF LEADING EDGE IMPACTS (CONT'D)

Shot No.	Target Material	Target Thickness At Point Of Impact (mm)	Target Support Method	Projectile Type	Projectile Size (mm)	Impact Velocity (m/s)	Type of Impact	Remarks
8329	Ti 8-1-1	0.23	Cantilever	Silica Sand	1.00 to 1.19	429.2	30° on edge	Multiple impacts with 6 on edge which generated a pitted edge with some material loss and permanent deformation of 0.8mm
8330	Ti 8-1-1	0.23	Cantilever	Pyrex Beads	1.59	484.3	30° on edge	4 impacts with 2 on edge some loss of material and permanent deformation of 0.5mm
8331	Ti 8-1-1	0.23	Cantilever	Pyrex Beads	1.59	455.1	30° on edge	3 impacts with 2 on edge, some loss of material and permanent deformation of 0.4mm
8332	Ti 8-1-1	0.23	Cantilever	Glass Beads	0.50 to 0.59	442.0	30° on edge	Multiple impacts which generated a peened edge and permanent deformation of 0.2mm
8333	Ti 8-1-1	0.23	Cantilever	Glass Beads	0.50 to 0.59	418.5	30° on edge	Multiple impacts which generated a peened edge and permanent deformation of 0.3mm
8334	Ti 8-1-1	0.23	Cantilever	Glass Beads	0.50 to 0.59	616.9	30° on edge	Bad Shot-Sabot impacted target
8335	Ti 8-1-1	0.20	Cantilever	Glass Beads	0.50 to 0.59	357.2	30° on edge	Multiple impacts which generated peened edge with some loss of material and permanent deformation of 0.5mm
8336	Ti 8-1-1	0.20	Cantilever	Glass Beads	0.50 to 0.59	492.6	30° on edge	Multiple impacts which generated a peened edge with some loss of material and permanent deformation of 0.5mm
8337	Ti 8-1-1	0.25	Cantilever	Glass Beads	0.25 to 0.30	474.3	30° on edge	Multiple impacts which generated a peened edge with permanent deformation of 0.1mm
8338	Ti 8-1-1	0.25	Cantilever	Glass Beads	0.25 to 0.30	378.0	30° on edge	Multiple impacts which generated a peened edge with permanent deformation of 0.1mm
8339	Ti 8-1-1	0.25	Cantilever	Glass Beads	0.25 to 0.30	468.8	30° on edge	Multiple impacts which generated a peened edge with permanent deformation of 0.1mm

TABLE 1. SUMMARY OF TEST CONDITIONS FOR PRELIMINARY SHOTS AND FIRST SERIES OF LEADING EDGE IMPACTS (CONT'D)

Shot No.	Target Material	Target Thickness At Point Of Impact (mm)	Target Support Method	Projectile Type	Projectile Size (mm)	Impact Velocity (m/s)	Type of Impact	Remarks
8351	Ti 8-1-1	0.23	Cantilever	Pyrex Beads	1.59	313.9	10° on edge	3 edge impacts, some loss of material and permanent deformation of 0.3mm
8352	Ti 8-1-1	0.23	Cantilever	Pyrex Beads	1.59	495.0	10° on edge	5 impacts, 2 on edge, some loss of material and permanent deformation of 0.5mm
8353	Ti 8-1-1	0.23	Cantilever	Pyrex Beads	1.59	501.1	10° on edge	3 impacts on edge, some loss of material and permanent deformation of 0.2mm
8354	Ti 8-1-1	0.23	Cantilever	Silica Sand	1.00 to 1.19	307.8	10° on edge	2 impacts on edge, some loss of material and permanent deformation of 0.2mm
8355	Ti 8-1-1	0.23	Cantilever	Silica Sand	1.00 to 1.19	312.7	10° on edge	2 impacts on edge, some splitting and roll back with material loss and permanent deformation of 0.8mm
8356	Ti 8-1-1	0.23	Cantilever	Silica Sand	1.00 to 1.19	490.1	10° on edge	4 impacts, 2 on edge, some loss of material and permanent deformation of 0.6mm

TABLE 2. SUMMARY OF TEST CONDITIONS FOR FATIGUE TEST SPECIMEN IMPACTS*

Shot No.	Thickness at Impact Point (mm)	Projectile Type	Size (mm)	Support Method	Velocity (m/s)	Single Impact Nicks Width (mm)	Depth (mm)	Calc K_T	Remarks
8365	0.25	Pyrex bead	1.59		496.2	1.27	0.33	2.29	
8367	0.20	"	1.59		511.1	1.38	.525	2.71	
8368	0.20	"	1.59		485.5	1.17	.340	2.42	
8369	0.17	"	1.59		503.5	1.26	.383	2.47	
8370	0.25	"	1.59		455	1.14	.322	2.39	
8371	0.17	Glass bead	0.59 to 0.84		322.2	0.41	0.11	2.30	
8372	0.17	"	0.59 to 0.84		300.2	0.43	0.12	2.41	
8373	0.17	"	0.59 to 0.84		300.2	0.46	0.05	1.60	
8374	0.17	"	0.59 to 0.84		301.1	0.44	0.04	1.48	
8375	0.17	"	0.59 to 0.84		296.9	0.53	0.11	2.11	
8376	0.20	"	0.59 to 0.84		298.4	0.39	0.04	1.55	
8447	0.23	"	0.76 to 0.84		289.0	0.43	0.10		
8448	0.25	"	0.76 to 0.84		300.5	0.43	0.05		
8449	0.28	"	0.76 to 0.84		298.7	0.56	0.10		
8450	0.28	"	0.76 to 0.84		299.9	0.20	0.03		
8451	0.25	"	0.76 to 0.84		324.3				
8452	0.25	"	0.76 to 0.84		332.2	0.61	0.10		
8453	0.25	"	0.76 to 0.84		289.6	0.58	0.10		
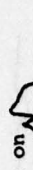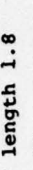
* Target material for all shots was Ti 8-1-1, all shots were at room temperature, impact angle was 30°, target size was 152.4 x 38.1 x 1.6.

TABLE 2. SUMMARY OF TEST CONDITIONS FOR FATIGUE TEST SPECIMEN IMPACTS*

Shot No.	Thickness at Impact Point (mm)	Projectile Type	Projectile Size (mm)	Support Method	Velocity (m/s)	Single Impact Nicks (mm) Width	Single Impact Nicks (mm) Depth	Calc K_T	Remarks	(mm)
8454	0.25	Glass bead	0.76 to 0.84		301.1	0.23	0.05			Edge on / Tear length 2.0
8455	0.25	"	0.76 to 0.84		299.6	0.58	0.11			Edge on
8432	0.25	Pyrex bead	0.25	Cantilever	232.3				Roll back with tear	Flat side down depth 0.8 width 2.7
8433	0.25	"	3.18	Cantilever	216.4				Roll back without tear	Edge on
8434	0.23	"	3.18	Cantilever	216.4				Nick in edge	Edge on depth 1.7
8435	0.25	"	3.18	Cantilever	216.1				Roll back without tear	Edge on
8436	0.23	"	3.18	Cantilever	216.1				Roll back without tear	Edge on
8437	0.25	"	3.18	Cantilever	216.1				Roll back with tear	Edge on / Tear length 1.2

* Target material for all shots was Ti 8-1-1, all shots were at room temperature, impact angle was 30°, target size was 152.4 x 38.1 x 1.6.

60

TABLE 2. SUMMARY OF TEST CONDITIONS FOR FATIGUE TEST SPECIMEN IMPACTS (CONT'D)*

Shot No.	Thickness at Impact Point (mm)	Projectile Type	Size (mm)	Support Method	Velocity (m/s)	Remarks	(mm)
8456	0.25	Pyrex bead	3.18	Cantilever	247.8	Roll back without tear	Edge on
8457	0.25	"	3.18	Cantilever	260.0	Roll back with tear	Edge on / Tear length 1.8
8438	0.25	"	1.59	Cantilever	227.4	Crease and slight bulge	Edge on
8439	0.25	"	1.59	Cantilever	239.0	Dent and slight bulge	
8440	0.25	"	1.59	Cantilever	274.6	Roll back without tear	Edge on
8441	0.25	"	1.59	Cantilever	327.7	Roll back with tear	Edge on
8442	0.25	"	1.59	Cantilever	307.8	Crease and bulge	Tear length 0.5 / Edge on

* Target material for all shots was Ti 8-1-1, all shots were at room temperature, impact angle was 30°, target size was 152.4 x 38.1 x 1.6.

61

TABLE 2. SUMMARY OF TEST CONDITIONS FOR FATIGUE TEST SPECIMEN IMPACTS (CONT'D) *

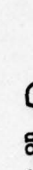| Shot No.	Thickness at Impact Point (mm)	Projectile Type	Projectile Size (mm)	Support Method	Velocity (m/s)	Remarks	(mm)
8443	0.25	Pyrex bead	1.59	Cantilever	335.3	Roll back without tear	Edge on
8444	0.28	"	1.59	Cantilever	367.0	Nicked the edge	Flat side down
8445	0.25	"	1.59	Cantilever	345.6	Nicked the edge	Flat side down
8446	0.25	"	1.59	Cantilever	343.2	Roll back with tear	Edge on / Tear length 0.5
8458	0.25	"	1.59	Cantilever	354.5	Nicked the edge	Flat side down
8459	0.25	"	1.59	Cantilever	346.9	Nicked the edge	Flat side down
8460	0.23	"	1.59	Cantilever	294.7	Roll back without tear	Edge on

* Target material for all shots was Ti 8-1-1, all shots were at room temperature, impact angle was 30°, target size was 152.4 x 38.1 x 1.6.

62

TABLE 3. SUMMARY OF TEST CONDITIONS TO STUDY EFFECT OF PROJECTILE SHAPE, VELOCITY, AND MATERIAL ON IMPACT DAMAGE

Shot No.	Material	Projectile Size (mm)	Projectile Shape	Velocity (m/s)	Target Dimensions (mm)	Target Material	Damage Evaluation
8498	Silica Sand	1.27-1.52	Irreg.	454	1.5x.381x.0163	Ti 8-1-1	Impact right of center-crater and bulge
8499	Silica Sand	1.27-1.52	Irreg.	534	same	Ti 8-1-1 Impact #2	Good impact-nicked the edge removing metal
8500	Silica Sand	1.27-1.52	Irreg.	409	same	Ti 8-1-1 Impact #3	Good impact-nicked the edge removing metal
8501	Silica Sand	1.27-1.52	Irreg.	290	same	Ti 8-1-1 Impact #4	Good impact-nicked edge removing metal
8502	Silica Sand	1.27-1.52	Irreg.	250	same	Ti 8-1-1 Impact #5	Good impact-pitted edge with bulge
8503	Silica Sand	1.27-1.52	Irreg.	196	same	Ti 8-1-1 Impact #6	Good impact-pitted edge with slight bulge
8504	Silica Sand	1.27-1.52	Irreg.	433	same	Ti 8-1-1	Good impact-nicked the edge removing metal
8505	Silica Sand	.51-.76	Irreg.	250	1.5x.381x.0160	Ti 8-1-1	Good impact-pitted edge with slight bulge
8506	Silica Sand	.51-.76	Irreg.	193	same	Ti 8-1-1 Impact #2	Good impact-pitted edge with slight bulge
8507	Silica Sand	.51-.76	Irreg.	150	1.5x.381x.0160	Ti 8-1-1 Impact #3	Good impact-nicked the edge
8508	Silica Sand	.51-.76	Irreg.	308	same	Ti 8-1-1 Impact #4	Good impact-pitted edge with bulge
8509	Silica Sand	.51-.76	Irreg.	159	same	Ti 8-1-1 Impact #5	Good impact-pitted the edge with slight bulge
8510	Silica Sand	.51-.76	Irreg.	456	same	Ti 8-1-1 Impact #6	Good impact-pitted the edge with bulge
8511	Silica Sand	.51-.76	Irreg.	199	same	Ti 8-1-1 Impact #7	Good impact-pitted edge with slight bulge

63

TABLE 3. SUMMARY OF TEST CONDITIONS TO STUDY EFFECT OF PROJECTILE SHAPE, VELOCITY, AND MATERIAL ON IMPACT DAMAGE (CONT'D)

Shot No.	Material	Projectile Size (mm)	Shape	Velocity (m/s)	Target Dimensions (mm)	Target Material	Damage Evaluation
8474	Chrome	0.79	Sphere	120.4	1.5x.381x.0163	Ti 8-1-1	Good impact-dent and bulge
8475	Chrome	0.79	Sphere	191.1	same	Ti 8-1-1 Impact #2	Good impact-dent and bulge
8476	Chrome	0.79	Sphere	243.5	same	Ti 8-1-1 Impact #3	Good impact-nick and bulge
8477	Chrome	0.79	Sphere	340.8	same	Ti 8-1-1 Impact #4	Good impact-nick and bulge
8478	Chrome	0.79	Sphere	313.1	same	Ti 8-1-1 Impact #5	Good impact-crease and bulge
8479	Chrome	0.79	Sphere	565.2	same	Ti 8-1-1 Impact #6	Good impact-nicked edge removing some metal
8480	Pyrex Bead	1.59	Sphere	143.9	1.5x.381x.0160	Ti 8-1-1	Good impact-dent and bulge
8481	Pyrex Bead	1.59	Sphere	206.4	same	Ti 8-1-1 Impact #2	Good impact-nicked the edge removing metal
8482	Pyrex Bead	1.59	Sphere	249.6	same	Ti 8-1-1 Impact #3	Good impact-nicked the edge removing metal
8483	Pyrex Bead	1.59	Sphere	290.5	1.5x.381x.0160	Ti 8-1-1 Impact #4	Good impact-nicked the edge removing metal
8484	Pyrex Bead	1.59	Sphere	419.5	same	Ti 8-1-1 Impact #5	Good impact-nicked the edge removing metal
8485	Pyrex Bead	1.59	Sphere	463.7	same	Ti 8-1-1 Impact #6	Good impact-nicked the edge removing metal
8486	Pyrex Bead	3.16	Sphere	128.3	1.5x.381x.0160	Ti 8-1-1	Good impact-nicked the edge removing metal
8487	Pyrex Bead	3.16	Sphere	187.5	same	Ti 8-1-1 Impact #2	Good impact-nicked the edge removing metal
8488	Pyrex Bead	3.16	Sphere	217.3	same	Ti 8-1-1 Impact #3	Good impact-crease and bulge
8489	Pyrex Bead	3.16	Sphere	290.5	same	Ti 8-1-1 Impact #4	Good impact-nicked the edge removing metal
8490	Pyrex Bead	3.16	Sphere	346.3	same	Ti 8-1-1 Impact #5	Good impact-crease and bulge

TABLE 3. SUMMARY OF TEST CONDITIONS TO STUDY EFFECT OF PROJECTILE SHAPE, VELOCITY, AND MATERIAL ON IMPACT DAMAGE (CONT'D)

Shot No.	Projectile Material	Size (mm)	Shape	Velocity (m/s)	Target Dimensions (mm)	Target Material	Damage Evaluation
8491	Pyrex Bead	3.16	Sphere	471.6	1.5x.381x.0160	Ti 8-1-1 Impact #6	Good impact-nicked the edge removing metal
8492	Glass Shot	0.76	Sphere	297.2	1.5x.381x.0163	Ti 8-1-1	Good impact-nicked edge removing metal
8493	Glass Shot	0.76	Sphere	246	same	Ti 8-1-1 Impact #2	Good impact-dent and bulge
8494	Glass Shot	0.76	Sphere	220	same	Ti 8-1-1 Impact #3	Good impact-dent and bulge
8495	Glass Shot	0.76	Sphere	196	same	Ti 8-1-1 Impact #4	Good impact-very slight dent
8496	Glass Shot	0.76	Sphere	412	same	Ti 8-1-1 Impact #5	Good impact-dent and bulge
8497	Glass Shot	0.76	Sphere	497	same	Ti 8-1-1 Impact #6	Good impact-dent and bulge

65

TABLE 4. SUMMARY OF TEST CONDITIONS FOR IMPACTS FROM DEBRIS

Shot No.	Material	Projectile Size (mm)	Post Test Proj.	Proj.	Velocity (m/s)	Target Dimensions (mm)	Target Material	Damage Evaluation
8512	Debris	1.09	#11	#1	320	1.5x.381 x.0160	Ti 8-1-1	Good impact-dent with bulge
8513	"	1.47	#11	#4	303	same	Ti 8-1-1 Impact #2	Good impact-nicked the edge removing metal
8514	"	1.55	#11	#5	309	same	Ti 8-1-1 Impact #3	Good impact-pitted the edge
8515	"	1.98	#11	#8	320	same	Ti 8-1-1 Impact #4	Good impact-dent with bulge and roll back
8516	"	2.11	#11	#9	304	same	Ti 8-1-1 Impact #5	Good impact-nicked the edge removing metal
8517	"	1.78	#11	#11	316	same	Ti 8-1-1 Impact #6	Impact off center to the right-pitting the surface
8518	"	1.04	#18	#7	316	1.5x.381 x.0163	Ti 8-1-1	Good impact-crease and bulge
8519	"	1.27	#18	#9	320	same	Ti 8-1-1 Impact #2	Good impact-nicked the edge removing metal
8520	"	1.57	#18	#12	311	same	Ti 8-1-1 Impact #3	Good impact-pitted edge with slight bulge
8521	"	2.21	#18	#6	314	1.5x.381 x.0163	Ti 8-1-1 Impact #4	Good impact-nicked the edge removing metal
8522	"	2.57	#18	#4	317	same	Ti 8-1-1 Impact #5	Good impact-pitted edge with slight bulge
8523	"	1.93	#18	#3	321	same	Ti 8-1-1 Impact #6	Good impact-pitted edge with slight bulge
8524	"	0.89	#23	#1	312	1.5x.381 x.0163	Ti 8-1-1	Good impact-pitted the edge
8525	"	1.22	#23	#7	329	same	Ti 8-1-1 Impact #2	Impact off center to the right-pitted surface
8526	"	2.26	#23	#5	323	same	Ti 8-1-1 Impact #3	Pitted surface with slight bulge- Proj. broke up resulting in multiple impacts

66

TABLE 4. SUMMARY OF TEST CONDITIONS FOR IMPACTS FROM DEBRIS (CONT'D)

Shot No.	Projectile Material	Size (mm)	Post Test Proj.	Velocity (m/s)	Target Dimensions (mm)	Target Material	Damage Evaluation
8527	Debris	2.34	#8	316	1.5x.381 x.0163	Ti 8-1-1 Impact #4	Good impact-nicked the edge removing metal
8528	Debris	2.84	#2	319	same	Ti 8-1-1 Impact #5	Good impact-pitted edge with bulge
8529	Debris	3.18	#6	328	same	Ti 8-1-1 Impact #6	Good impact-projectile broke up, nicked the edge

TABLE 5. SUMMARY OF TEST CONDITIONS FOR IMPACTS ON VARIOUS LEADING EDGE THICKNESSES

Shot No.	Material Ti 8-1-1	Size (mm)	Taper Leading Edge Thickness (mm)	Projectile Type	Projectile Size	Velocity (m/s)	Nick or Dent (mm) Width	Nick or Dent (mm) Depth	Remarks	
8568	Impact #1	152.4x38.1 x1.6	0.38	Pyrex bead	3.18	180.1	1.98	0.28	Roll back with tear	Edge on
8569	Impact #2	same	0.38	"	3.18	208.5	2.08	0.36	Nicked the edge	Flat side down
8570	Impact #3	same	0.38	"	3.18	221.0	2.16	0.10	Roll back	Edge on
8571	Impact #4	same	0.38	"	3.18	268.2	4.50	0.24	Roll back	Edge on
DIFFERENT SPECIMEN										
8572	Impact #1	same	0.38	"	3.18	264.6	2.44	0.50	Nicked the edge	Flat side down
8573	Impact #2	same	0.38	"	3.18	256.0	3.48	0.10	Roll back	Edge on
8574	Impact #3	same	0.38	"	3.18	286.5	2.11	0.41	Nicked the edge	Flat side down

*For all shots impact angle was 30°, cantilever support method. Taper leading edge was 4°.

TABLE 5. SUMMARY OF TEST CONDITIONS FOR IMPACTS ON VARIOUS LEADING EDGE THICKNESSES (CONT'D)

Shot No	Material Ti 8-1-1	Size (mm)	Taper Leading Edge Thickness (mm)	Projectile Type	Projectile Size	Velocity (m/s)	Nick or Dent (mm) Width	Nick or Dent (mm) Depth	Remarks	
8575	Impact #4	152.4x38.1 x1.6	0.38	Pyrex beads	3.18	296.9	2.17	0.97	Roll back	Flat side / down
DIFFERENT SPECIMEN										
8578	Impact #1	same	0.38	"	3.18	350.8	2.12	3.54	Roll back with tear	Flat side / down
8579	Impact #2	same	0.38	"	3.18	358.7	2.08	1.93	Roll back with tear	Flat side / down
8580	Impact #3	same	0.38	"	3.18	407.8	5.91	3.11	Roll back with tear	Flat side / down
DIFFERENT SPECIMEN										
8581	Impact #1	same	0.51	"	3.18	425.2	2.43	2.64	Nicked the edge	Flat side / down
8582	Impact #2	same	0.51	"	3.18	461.2	2.17	0.74	Roll back	Flat side / down
8583	Impact #3	same	0.51	"	3.18	335.3	2.26	0.84	Nicked the edge	Flat side / down

*For all shots impact angle was 30°, cantilever support method. Taper leading edge was 4°.

TABLE 5. SUMMARY OF TEST CONDITIONS FOR IMPACTS ON VARIOUS LEADING EDGE THICKNESSES (CONT'D)

Shot No.	Material Ti 8-1-1	Size (mm)	Taper Leading Edge Thickness (mm)	Projectile Type	Projectile Size	Velocity (m/s)	Nick or Dent (mm) Width	Depth	Remarks	
DIFFERENT SPECIMEN										
8584	Impact #1	152.4x38.1 x1.6	0.51	Steel spheres	3.18	192.0	2.21	0.28	Roll back	Edge on
8585	Impact #2	same	0.51	Steel spheres	3.18	246.9	3.10	1.75	Roll back penetration	Flat side down
8586	Impact #3	same	0.51	Steel spheres	3.18	290.5	6.35	3.23	Roll back penetration	Edge on
8587	Impact #4	same	0.51	Steel spheres	3.18	506.6	3.18	3.35	Complete penetration	Flat side down
8588	Impact #1	same	0.51	Steel spheres	3.18	375.8	3.21	3.53	Complete penetration	Edge on
DIFFERENT SPECIMEN										
8589	Impact #1	same	0.51	Steel	1.59	255.4	1.24	0.28	Nicked the edge	Flat side down
8590	Impact #2	same	0.51	Steel spheres	1.59	362.7	2.18	1.12	Roll back crease with tear	Edge on

*For all shots impact angle was 30°, cantilever support method. Taper leading edge was 4°.

TABLE 5.   SUMMARY OF TEST CONDITIONS FOR IMPACTS ON VARIOUS LEADING EDGE THICKNESSES (CONT'D)

Shot No.	Material Ti 8-1-1	Size (mm)	Taper Leading Edge Thickness (mm)	Projectile Type	Size	Velocity (m/s)	Nick or Dent (mm) Width	Depth	Remarks	
8604	Impact #1	152.4x38.1 x3.175	0.76	Steel sphere	6.35	171.3	1.24	2.21	Roll back and crack	Edge on
8605	Impact #2	same	0.76	Steel sphere	6.35	150.9	0.68	0.51	Roll back and crack	Edge on
8606	Impact #2	same	0.76	Pyrex sphere	6.35	211.2	0.32	0.43	Nicked edge	Edge on

*For all shots impact angle was 30°, cantilever support method. Taper leading edge was 4°.

71

TABLE 5. SUMMARY OF TEST CONDITIONS FOR IMPACTS ON VARIOUS LEADING EDGE THICKNESSES (CONT'D)

Shot No.	Material Ti 8-1-1	Size (mm)	Taper Leading Edge Thickness (mm)	Projectile Type	Projectile Size	Velocity (m/s)	Nick or Dent (mm) Width	Nick or Dent (mm) Depth	Remarks	
8598	Impact #4	152.4x38.1	0.51	Steel sphere	1.59	349.0	1.22	0.33	Nicked edge	Flat side down
8599	Impact #5	same	0.51	Steel sphere	1.59	292.6	1.42	0.48	Nicked edge	Flat side down
DIFFERENT SPECIMEN										
8576	Impact #1	same	0.51	Pyrex sphere	6.35	179.5	1.02	0.55	Roll back	Edge on
8577	Impact #2	same	0.51	Pyrex sphere	6.35	235.9	1.19	0.56	Roll back	Edge on
DIFFERENT SPECIMEN										
8600	Impact #1	same	0.51	Steel sphere	6.35	240.5	1.46	4.62	Complete penetration	Edge on
8601	Impact #2	same	0.51	Steel sphere	6.35	185.9	0.47	1.14	Nicked edge	Edge on
8602	Impact #1	152.4x38.1 x3.175	0.76	Steel sphere	6.35	176.2	1.40	0.33	Roll back and crack	Edge on
8603	Impact #2	same	0.76	Steel sphere	6.35	192.3	0.57	2.13	Complete penetration	Flat side down

* For all shots impact angle was 30°, cantilever support method. Taper leading edge was 4°.

72

TABLE 5. SUMMARY OF TEST CONDITIONS FOR IMPACTS ON VARIOUS LEADING EDGE THICKNESSES (CONT'D)

Shot No.	Material Ti 8-1-1	Size (mm)	Taper Leading Edge Thickness (mm)	Projectile Type	Projectile Size	Velocity (m/s)	Nick or Dent Width (mm)	Nick or Dent Depth (mm)	Remarks	
8591	Impact #3	152.4x38.1	0.51	Steel sphere	1.59	608.7	1.12	1.71	Sabot impacted specimen	Flat side
8592	Impact #1	same	0.38	Steel sphere	1.59	503.8	2.24	0.10	Nick in edge	Flat side down
8593	Impact #2	same	0.38	Steel sphere	1.59	641.3	1.27	1.73	Complete penetration	Flat side down
8594	Impact #3	same	0.38	Steel sphere	1.59	434.9	1.19	1.91	Roll back with crease	Flat side down
DIFFERENT SPECIMEN										
8595	Impact #1	same	0.51	Steel sphere	1.59	509.3	1.17	2.03	Complete penetration	Flat side down
8596	Impact #2	same	0.51	Steel sphere	1.59	395.9			Nicked edge	Flat side down
8597	Impact #3	same	0.51	Steel sphere	1.59	381.9	1.55	0.76	Complete penetration	Flat side down

*For all shots impact angle was 30°, cantilever support method. Taper leading edge was 4°.